How and why small volcanic ocean islands collapse and move vertically up and down

Fernando O Marques, Luísa Ribeiro, Christian Hübscher, Ana C G Costa, Anthony Hildenbrand

scientific reports

Check for updates

OPEN

How and why small volcanic ocean islands collapse and move vertically up and down

Fernando O. Marques[1]✉, Luísa P. Ribeiro[1], Christian Hübscher[2], Ana C. G. Costa[3] & Anthony Hildenbrand[4]

Mass controls two major processes in volcanic islands: large-scale collapse and vertical movements. Therefore, large islands like Hawaii are gradually subsiding and have undergone massive landsliding. What if the mass is much smaller, and there is good evidence that the vertical movement is more complex than simple loading-related subsidence? Here, we show that small volcanic islands, seemingly stable because of the small mass, can undergo sector collapses that can affect the vertical movement of the island. Santa Maria Island (Azores) is ca. 170 times smaller than Hawaii; however, it has collapsed more than once, as inferred from new onshore and marine geophysical data. From the vertical distribution of submarine and subaerial lavas, we can infer a complex subsidence and uplift history (seamount-island-seamount-island, meaning that Santa Maria has been an island twice), which is most likely the consequence of alternating volcanic construction (loading = subsidence) and large-scale destruction by sector collapse (unloading = uplift). Given the age difference between Santa Maria and the underlying oceanic crust, the island likely sits on several hundred meters of marine sediments that could behave as a weak layer (detachment) under shear. We evaluate the likely collapse mechanism by numerical modelling and conclude that small volcanic islands can collapse when both the edifice and its substrate are weak. The proximity of Santa Maria to the East Azores Fault, active during the volcanic lifetime of Santa Maria, may point to the trigger mechanism of the flank collapses. The inferred instability factor, a weak substrate, could be responsible for similar evolutions in other volcanic ocean islands sitting on sediments overlying the igneous oceanic crust.

Keywords Santa Maria Island, Azores, Vertical movement, Sector collapse, Basement detachment, Numerical modelling, Marine geophysical data

Until relatively recent times (e.g., Refs.[1–4]), the destruction of volcanic ocean islands was thought to be mostly by meteoric (onshore) and marine (coastal) erosions. However, since the first recognition of a large-scale collapse in a volcanic island[1], evidence has shown that catastrophic collapses can massively erode the volcanic edifice in one event alone. This is well established for large islands, but is it true for small islands too? If it is, how and why does it happen, and what are the consequences regarding vertical movements?

The Big Island in the Hawaiian Ridge is the tallest relief on Earth. Therefore, its mass is large, which carries two major consequences: (1) a significant bending of the underlying elastic lithosphere, which is responsible for the continued subsidence of the island; (2) gravitational instability that has produced giant landslides (e.g. Refs.[1,2]). Volcanic construction and subsidence represent the most typical evolution of a large volcanic island: submarine lavas (seamount stage) are followed by subaerial lavas (island stage), which gradually become partially submerged due to subsidence. Everything seems straightforward in big islands: the lava sequence is simple, and they collapse due to the large mass. The opposite end-member is represented by small islands like Santa Maria Island in the Azores (Fig. 1), whose mass is ca. 170 times smaller than the mass of the Big Island. Based on mass alone, the main driver of gravitational instability, one would infer that the Big Island would collapse easily, but not Santa Maria. However, there is good evidence that Santa Maria has collapsed twice. Despite the much smaller mass, Santa Maria should also subside and exhibit the typical submarine-to-subaerial lava sequence observed in volcanic ocean islands when they evolve from a seamount to an island. However, as reported here, the lava sequence is not that simple, it is more complex, with submarine lavas intercalated with subaerial lavas, thus

[1]EMEPC – Task Group for the Extension of the Continental Shelf, Paço de Arcos, Portugal. [2]Institute of Geophysics, University of Hamburg, Hamburg, Germany. [3]Institut für Geothermisches Ressourcenmanagement, Bingen, Germany. [4]GEOPS, Univ. Paris-Sud, CNRS, Université Paris-Saclay, Orsay 91405, France. ✉email: fomarques@gmail.com

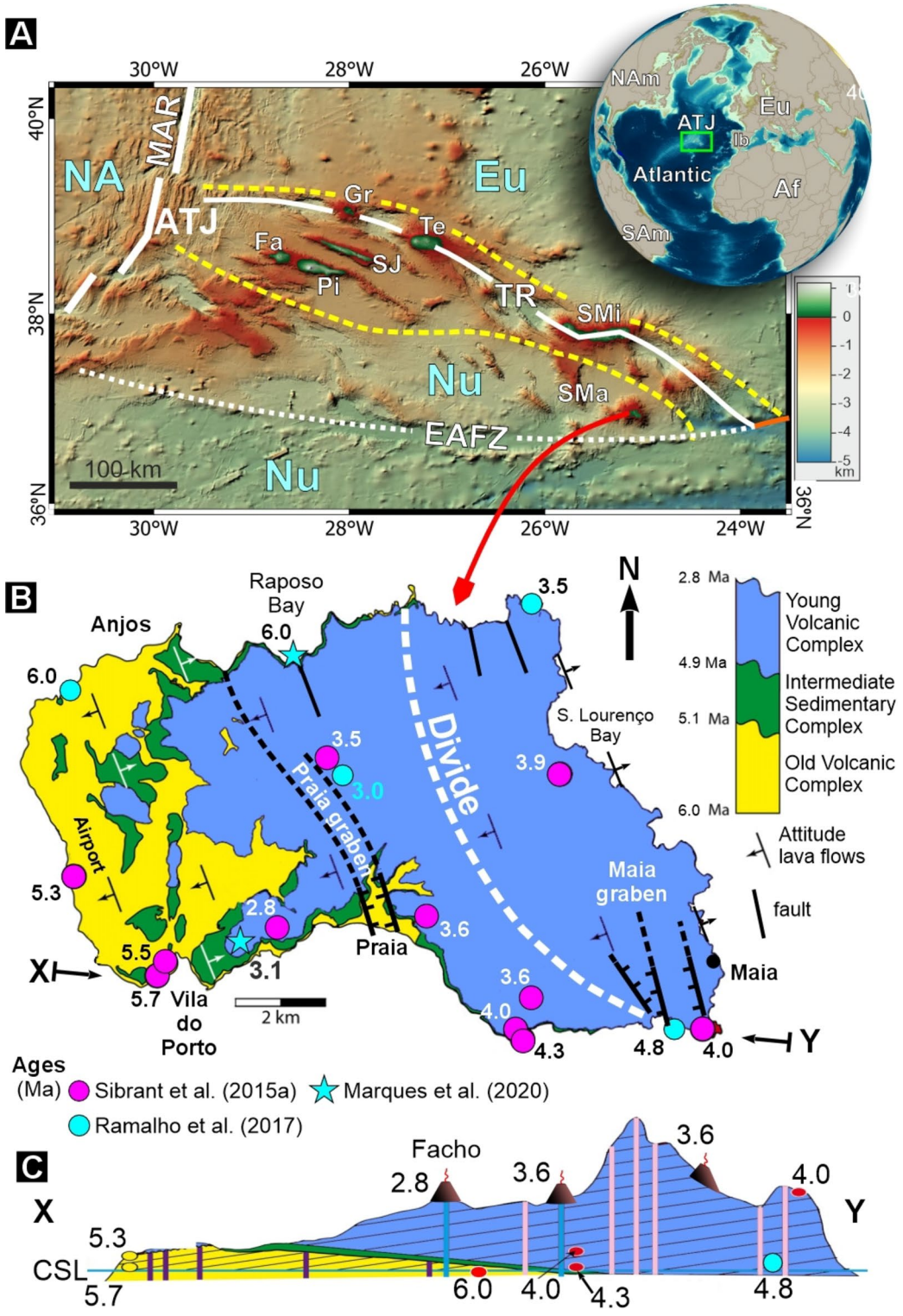

Fig. 1. (**A**) Tectonic setting of the Azores Triple Junction (ATJ) with the main tectonic and volcanic elements: three lithospheric plates, North America (NA), Eurasia (Eu), and Nubia (Nu); the Mid-Atlantic Rift (MAR); the Terceira Rift (TR); the East Azores Fracture Zone (EAFZ), the former boundary between the Eu and Nu plates. The Azores archipelago comprises nine islands, from W to E: Flores (Fl), Corvo (Co), Faial (Fa), Pico (Pi), S. Jorge (SJo), Graciosa (Gr), Terceira (Te), S. Miguel (SMi) and Santa Maria (SMa). The dashed yellow line delimits the diffuse Eu/Nu plate boundary. (**B**) Simplified Santa Maria geological map with main ages, faults, and attitude of lava flows. Note the curved divide concave to the east. (**C**) Geological profile along the southern coast (marked X–Y), similar to what is observed on the northern coast.

hinting at a complex evolution. Additionally, submarine lavas are currently observed above sea level, and locally up to 200 m altitude.

Flank collapses on oceanic islands are catastrophic events involving the sudden and massive failure of volcanic slopes, leading to landslides and potentially tsunamis. These collapses have significant geological and environmental consequences. Key instability factors and mechanisms that trigger these events include gravitational instability (e.g. mass loading, weak and/or inclined substrate, and over steepening[5–10]), volcanic activity (e.g. magma intrusion, eruptions and caldera collapse[11–16]), seismic activity[13,17–19], hydrothermal alteration and chemical weathering[20–22], pre-existing structural weaknesses (e.g. faults and fractures, and anisotropic rock properties affecting their strength[21,23,24]), climate and sea level changes[25–28], and composite triggers[29]. Understanding these mechanisms is vital for assessing the risks associated with volcanic islands and developing early warning systems to mitigate potential impacts. Continuous research and monitoring are essential for improving predictive models and enhancing community resilience. Here, we focus on one instability factor, substrate weakness, and use it in numerical simulations designed to show how and why Santa Maria can have undergone full-sector collapses.

The Azores volcanic province is a target of particular interest to investigate gravitational destabilisation and vertical movements because, unlike large intra-plate volcanic ocean islands developed on deep abyssal plains (e.g. in Hawaii, the western Canary, Reunion, or Tahiti), most of the Azores islands have a modest total height (less than 2500 m from the seafloor). An edifice height of 2500 m was considered a threshold value[30] because major gravitational destabilization episodes were only rarely observed for edifices with sizes below that value. However, since the first flank collapse recognized in Pico Island[31], more than twelve other flank collapses with individual volumes in the order of a few cubic kilometres have been recognized in the Azores from on and offshore studies[32–46]. This makes the archipelago a very special case to investigate further why and how small volcanic islands experience full-flank failures with associated complex vertical motions. The Santa Maria volcanic edifice is < 2500 m tall and lay on a tectonically active setting before 2.8 Ma. From onshore evidence, mostly the missing summits and eastern flanks of two main shield volcanoes, two SE-directed full-flank sector collapses have been proposed[36,38,43]. Here, we build on these earlier studies and add (1) new and critical onshore evidence for collapse and significant change in volcanic style, (2) new marine geophysical data (bathymetry and seismic profiles), and (3) new evidence for a complex history of vertical movements (an island that has been an island twice).

Santa Maria Island in the Azores is an ideal example to address these questions, because: (1) it is a small volcanic island with reduced mass compared to large islands like Hawaii; (2) the internal structure of Santa Maria's edifice is asymmetric (Fig. 2), comprising mostly W-dipping successions that may represent the remains of multiple episodes of eastward destruction, likely by massive full-sector collapses[38–43]; (3) the preserved stratigraphy of the island shows multiple alternating sub-aerial and submarine units; (4) submarine units at an

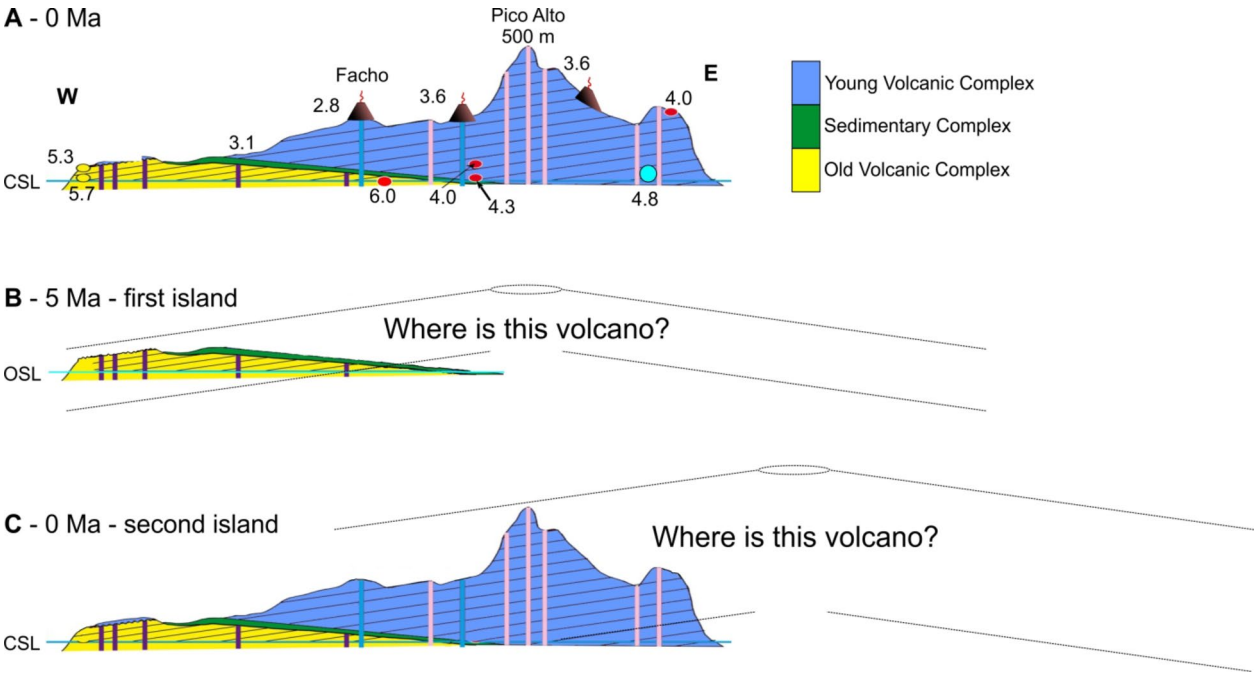

Fig. 2. Geological cross-sections along Santa Maria's southern coast at different times. (**A**) Present-day cross-section with the necessary reference information. Numbers represent ages in Ma. CSL and OSL mean current and old sea levels, respectively. (**B**) Cross-section representing Santa Maria ca. 5 Ma ago, before the deposition of the Young Volcanic Complex, from which we can infer that most of the original shield volcano is missing (only a small part has survived before the deposition of sediments). (**C**) Current cross-section showing that more than half of the young volcano is also missing.

altitude up to 200 m cannot be explained by sea level variations, thus pointing to significant uplift at some critical stages of the island's lifetime. Therefore, Santa Maria is an outstanding target, which can guide the study of other islands with similar records. The main purpose of this study was to investigate (1) the vertical movements of a small volcanic ocean island, (2) how and why it can undergo full-sector collapse, and (3) the possible relations between vertical movements and large-scale collapses.

Geological background

The Azores islands sit on a particular geodynamic setting, the Azores Triple Junction (ATJ, Fig. 1), where the North America, Eurasia and Nubia plates meet. The region is frequently shaken by earthquakes ($M < 7.0$) along the main tectonic structures, i.e. the Mid-Atlantic Rift and the diffuse boundary between the Eurasian and Nubian plates[47,48]. Although with moderate magnitude, some earthquakes can be very destructive when they occur at shallow depths, thus possibly acting as a trigger of flank collapse.

Santa Maria, the oldest island in the Azores, sits close to the East Azores Fracture Zone (Fig. 1), which is currently inactive but was the Eurasia-Nubia plate boundary before ca. 2.5 Ma ago. The plate boundary since ca. 2.5 Ma has been the Terceira Rift[37,44,49], which lies north of Santa Maria (Fig. 1). The evolution of subaerial Santa Maria[38,43,50] (see Fig. 1B, C) started ca. 6 Ma ago with a basaltic subaerial shield volcano (Old Volcanic Complex), which collapsed to the east at ca. 5.1 Ma[36,38,43]. A sedimentary unit, the Intermediate Sedimentary Complex, has been deposited on a major unconformity atop the Old Volcanic Complex. A new basaltic shield volcano (Young Volcanic Complex) grew on the collapse scar, initially submarine and later subaerial as it grew out of the water; this second volcano then collapsed to the east at ca. 3.9 Ma[36,38,43]. Following the collapse, numerous Strombolian cones grew unconformable on the concave scarp facing east, from ca. 3.7 to 2.8 Ma, thus blanketing the collapse scar. The distribution and geometry of these units are well illustrated on the geological map and the cross-section in Fig. 1B, C. This simple volcanic stratigraphy can be more complex, with three volcanic complexes instead of two (Old, Intermediate and Young volcanic complexes), if we consider that the post-second collapse Strombolian cones comprise a new volcanic complex, which could be called Young Volcanic Complex. Then, the current Young Volcanic Complex would be renamed the Intermediate Volcanic Complex.

During Santa Maria's lifetime, sea level changes have been characterised by major low stands (ca. − 130 m below current sea level) and no significant high stands (< 20 m)[51,52]. Similarly to other volcanic ocean islands[53–55], Santa Maria experienced considerable vertical motions that cannot be explained by sea level fluctuations[38,43,50], and are witnessed by intercalations of subaerial and submarine lavas, and submarine lava flows currently outcropping up to an altitude of ca. 200 m.

The topography of Santa Maria (Fig. 3A) shows a well-defined divide, separating the contrasting topography between E (rugged and concave to the E) and W (convex structural surface gently dipping to the W, similar to the lava flows of the two volcanic complexes) Santa Maria.

Methods

For the present work, we used: (1) fieldwork to map volcanic cones on the E half of the island, where they occur on an eastward concave surface E of the divide (Fig. 3A), and to measure the attitude of lava flows, which allows confirming the position of Strombolian cones and recognizing where flanks are missing; (2) high-resolution bathymetry to identify debris deposits; (3) seismic reflection profiles to distinguish between stable and collapsed slopes of Santa Maria; and (3) numerical modelling to address the mechanics of gravitational failure of volcanic edifices that can lead to a full-flank sector collapse in small islands.

New on and offshore data

The main argument used for the identification of the two large-scale flank collapses in Santa Maria[36,38,43] is that the summits and eastern flanks of the two main shield volcanoes are missing (only the western flank is preserved above sea level; cf. Figs. 2 and 3B). The collapse scar was subsequently buried by young volcanic cones, which were systematically mapped for this work.

Reference[56] suggested that "… *seacliffs previously attributed to marine erosion of many additional islands may instead be headwalls of still other landslides. These landslides occur in a wide range of settings and probably represent only a small sample from a large population*". This is the procedure we followed in the present work: we first analysed the island morphology (mostly looking for large-scale embayments), and then we collected geological and available geochronological data to put in evidence the large-scale unconformities that cannot be explained by simple meteoric or marine erosion.

From the geological evolution of Santa Maria, two debris-avalanche deposits, separated by a volcanic layer, should exist at the sea bottom southeast of the island. Marine campaigns have focused mostly on the shallow platform surrounding the island, but these are not relevant to the study of landslides that occurred more than 3.5 Ma ago. In particular, the sea bottom surrounding Santa Maria has not been considered, despite being the preferential locus for the accumulation of large-scale debris-avalanche deposits, as observed around the other Azores islands[30,40–42,44] and around many other volcanic islands[2,4,57–64].

We present new offshore topographic and seismic data, which can help us discern mass remobilization generated by the two inferred east-directed flank collapses. Bathymetric data used in this study was compiled from different sources (Fig. S1). The multibeam bathymetry data was acquired by the Task Group for the Extension of the Continental Shelf (EMEPC) using an EM120 Multibeam Echosounder (MBES) onboard the research vessels *N.R.P. Almirante Gago Coutinho*, *N.R.P Dom Carlos* and *R/V Kommandor Jack*, between 2006 and 2014, within the scope of the Portuguese project for the Extension of the Continental Shelf, complying with Order 2 (intended for areas where the water depth is such that a general depiction of the seabed is considered adequate) from IHO (International Hydrographic Organization) standards (cf. https://iho.int/uploads/user/pu

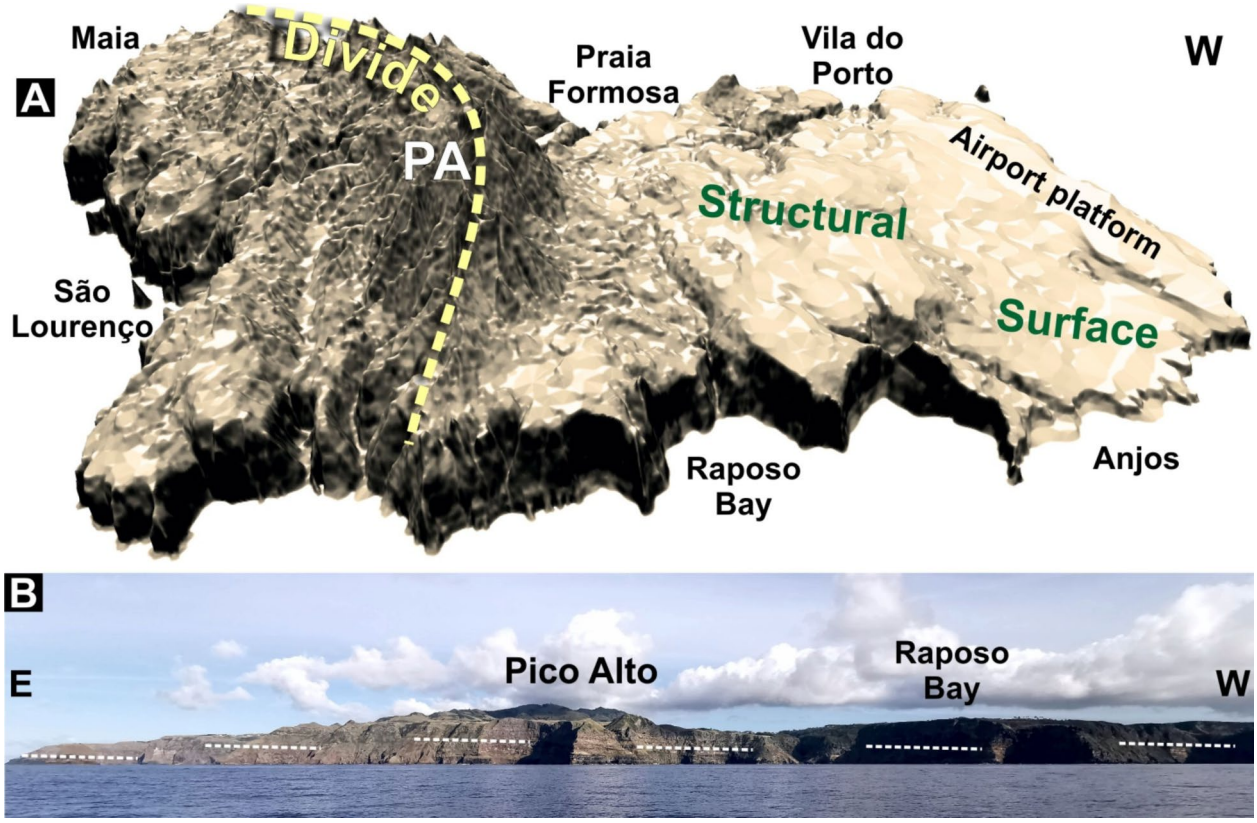

Fig. 3. (**A**) 3-D shaded relief viewed from N and showing the position of the divide and the contrasting topography between E (rugged and concave to the E) and W (structural surface gently dipping to the W, similarly to the lava flows of the two volcanic complexes) Santa Maria. The drawn divide separates the two main drainage basins, in this case to the east and to the west. (**B**) Panorama photograph of the entire northern seaboard with lava flows gently dipping to the W (highlighted by dashed white lines), similar to the southern seaboard.

bs/standards/s-44/S-44_Edition_6.1.0.pdf). MBES data were processed using CARIS HIPS&SIPS™ software at the Hydrographic Institute of Portugal to produce the image shown in Fig. S1. We also searched the European Marine Observation Data Network[65] (EMODnet) bathymetry repository for high-resolution data, which we downloaded in XYZ format from the EMODnet bathymetry Portal to produce the image shown in Fig. S1. The MBES bathymetry data were used to generate digital elevation models (DEM) at spatial resolutions from 100 to 150 m. The multi-resolution DEMs were also used to generate regional sun-shaded image renders and perspective views, and to extract bathymetric profiles using Fledermaus™ software to interpret the submarine landscapes. Bathymetric full-coverage images show the multi-resolution MBES data overlapped on GEBCO Compilation Group 2019 bathymetric data available in this area with a spatial resolution of 15 arc seconds[66]. Other bathymetric data were used from Ref.[67].

The bathymetric data are complemented by three seismic profiles acquired in 2014 offshore Santa Maria during the M113 cruise onboard the German research vessel *R/V Meteor*[68]. The here presented seismic data were generated by using an array of three GI-Guns and one Mini-Gun (150 cubic inch total primary volume) as the seismic source, and were recorded with a 144-channel streamer (active length: 600 m). The dominant frequency was around 80–100 Hz. Further technical details on seismic data acquisition and processing can be found in Ref.[68].

Numerical modelling

The numerical simulations reported here serve only as proof of concept; a full numerical approach in 3-D deserves more than one full publication, which is not the objective here.

If the early Santa Maria seamount is < 8 Ma (6 Ma above sea level), and the oceanic crust below Santa Maria is ca. 40 Ma old (magnetic anomaly 18–20, cf. Ref.[69]), then Santa Maria sits on an oceanic crust covered by marine sediments accumulated over a period of ca. 30 Ma. Based on seismic reflection and refraction data, Ref.[70] calculated a maximum sediment thickness of 1500 m between São Miguel and Santa Maria. Reference[71] estimated the thickness of sediments on 30 Ma basaltic crust to be about 650–700 m, assuming interval velocities of 1.8–2 km/s for a two-way travel time of ca. 0.7 s for the sediments. Hence, Santa Maria most likely sits on a pile of sediments of similar thickness. What are the effects of such a basal sedimentary pile on the gravitational stability of a small volcanic ocean island, especially regarding edifice spreading and flank collapse? Is a soft base

capable of detachment, thus facilitating full-flank sector collapse? Here we use numerical modelling to address this specific question. We distinguish between full and partial flank sector collapse because the mechanics of the two processes are different, as indicated by the numerical simulations. We further use new on and offshore data (bathymetry and reflection seismic profile) to track potential collapse structures and deposits generated by the putative flank collapses, which may provide additional insight into landslide mechanisms and debris-avalanche propagation.

Knowing that the shape of a typical volcanic edifice is a cone, one expects to find a gradient of temperature and pressure from the rim (both lower) to the centre (both higher) of the base below the cone's vertex. Therefore, the rheology of the basal sediments should vary from the rim (soft) to the core (hard metamorphic rock), but the effects of pressure and temperature on the rheology of sediments underlying the island should depend on the island's size. Given that our main goal was to investigate the effects of partial or total detachment at the base of the volcanic edifice, in the present work we used a small edifice and low viscosity rheology in a ring totally or partially occupying the base of the volcanic edifice.

The numerical simulations were executed with the 2-D Finite Element Method code MVEP2[72,73], which allows for failure without a prescribed weakness seed. We ran models that included a 100 m thick weak layer totally or partially underlying the volcanic edifice, which was 40 km wide and 3.5 km tall as in Santa Maria.

For simplification, the density (ρ) was kept constant at 2700 kg/m^3 for all phases, although in nature the density of sediment is generally lower than that value (ρ = 2100–2200 kg/m^3 for 0-1700 m thick deposits; Ref.[74] and references therein); cohesion, C, was kept at 1 MPa for the volcanic edifice and basal weak layer, because the former is pervasively fractured and/or porous, and the latter is unconsolidated and soft sediment. We considered for the weak basal layer: viscosity, $\eta = 10^{18}$–10^{19} Pa s, values within the range published for clay material; and angle of internal friction, φ = 15°, close to the value used by Ref.[75] (φ = 16°), but the clay material could be even weaker if under fluid overpressure[76]. We ran simulations varying η and φ of the volcanic edifice (10^{21}–10^{23} Pa s, 15°–30°, respectively). The parameter values used in the numerical simulations are summarised in Table 1.

Results

New field data

Important outstanding questions still require an explanation at Santa Maria if we want to understand its evolution and use it as an example to study other volcanic ocean islands. In particular, a few outcrops record critical pieces of Santa Maria's evolution that can be very helpful when trying to find explanations for the observations gathered during fieldwork. Such outcrops are of easy access, very well exposed, and occur in critical sectors of the island: (1) Pedreira do Campo (Fig. 4) for the evolution before ca. 5 Ma, and (2) well-exposed volcanic cones on eastern Santa Maria (Fig. 5) for the evolution after ca. 5 Ma.

At Pedreira do Campo, we can observe an exposed sequence of marine sediments at the base, followed upwards by submarine pyroclastic deposits (hyaloclastites) and lava flows (pillow lavas) (Fig. 4A). At the local scale, all lithotypes are submarine and seem to be in depositional continuity, without clear evidence of a major erosion surface (unconformity). Walking down to the sea from Facho (Fig. 4B), we can observe the sequence of rocks represented in Fig. 4C, i.e. subaerial lavas of the Young Volcanic Complex at the top (the Facho volcanic cone), followed downwards and without apparent unconformity by submarine lavas, then by marine sediments, and finally by subaerial lavas of the Old Volcanic Complex. At the local scale, it is clear that the lava flows of both the Young and Old Volcanic Complexes dip gently to the west (Fig. 2). At the scale of the island, it seems clear that the marine sediments dip in the opposite sense, i.e. to the east, because they are observed at Pedreira do Campo at ca. 100 m altitude, and further east at sea level (cf. Fig. 1B, C). From these observations, we conclude that the Old Volcanic Complex is covered in unconformity by the marine sediments, supporting a major truncation of the basal subaerial lava flows before the deposition of the overlying marine sediments. From these observations, some questions critical to the understanding of Santa Maria's evolution arise (Figs. 2 and 4) concerning the location and meaning of major unconformities (between subaerial lavas and overlying marine sediments, or between these and submarine lavas); the mechanism that can put submarine sediments and lavas on top of subaerial lavas; and where we would put the summit and eastern flanks of the older and younger volcanoes (Figs. 2 and 4).

On the eastern flank of the Island, we can observe many Strombolian cones, some of which preserve the original shape exceptionally well (for their age) and have their interiors well exposed (cf. Fig. 5). While the Strombolian cones in the west are only a few and lie on an outward convex topography, as one would expect for adventitious cones, the more than one hundred cones in the east lie on an outward concave surface, the opposite of what is expected in a non-collapsed shield volcano (convex outward), which raises two main questions: (1) knowing that the geometry of a volcanic cone is convex outward, then how can we explain so many cones on a concave surface? (2) Why are there so many cones in the east, the smallest part of Santa Maria, and so few in the west, the largest part of the Island?

Density (kg/m^3)	Cohesion (MPa)	Viscosity basal layer (Pa s)	Viscosity volcanic edifice (Pa s)	Angle internal friction basal layer (°)	Angle internal friction volcanic edifice (°)
2700	1	10^{18}–10^{19}	10^{21}–10^{23}	15	15–30

Table 1. Parameter values used in the simulations.

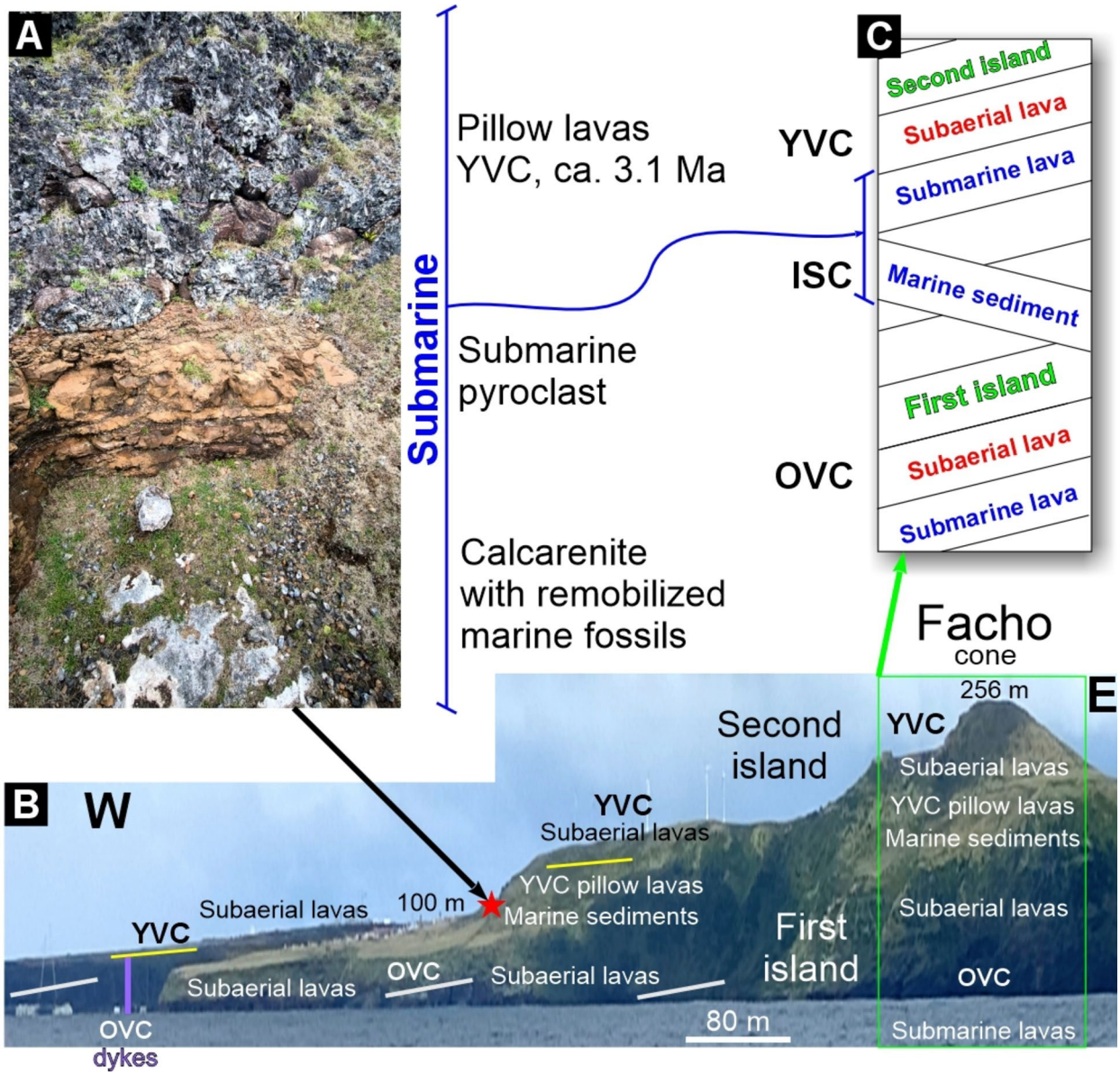

Fig. 4. Image synthesising the geological features observed in southwestern Santa Maria, from Vila do Porto to Praia (Fig. 1B), from which several critical questions arise: in the observed section, where is the main unconformity? Why has volcanism changed from subaerial back to submarine? Where are the eastern flanks and summits of the two main volcanic complexes?. (**A**) Photograph of the rock sequence exposed at Pedreira do Campo geosite (marked with a red star in B). (**B**) 3-D Google view of Santa Maria's southwestern coast on which the critical stratigraphy is drawn. White and yellow lines represent the dips of OVC (Old Volcanic Complex) and YVC (Young Volcanic Complex) lava flows, respectively. (**C**) Schematic representation of the area marked by the green rectangle in (**B**) to highlight the alternating subaerial and submarine volcanic and sedimentary rocks. Note that subaerial lavas of the Old Volcanic Complex lie below submarine sediments and lavas of the ISC (Intermediate Sedimentary Complex) and Young Volcanic Complex, respectively, which is the opposite of what is expected in a volcanic island born as a seamount–submarine seamount to subaerial island. This sequence is more complex and means that Santa Maria has been an island twice.

The new mapping of Strombolian cones can seem of minor importance at first glance, and that is probably the reason why they have never been recognised and mapped systematically. Only a couple of the largest cones in eastern Santa Maria appear on the geological map[77]. However, they are critical for the study of Santa Maria because they are many in the eastern third of the island and sit on a concave surface, which is not the typical convex surface of a shield volcano. The age of these cones sets a limit to the age of the concave surface, which is critical for its interpretation. The recognition of these cones is also important because they mark a great change in volcanic style, as recognised in other volcanic ocean islands[78,79]. Despite their age (ca. 2.8–3.6 Ma), most Strombolian cones in Santa Maria have their original shape well recognizable (cf. Fig. 5), and can thus be

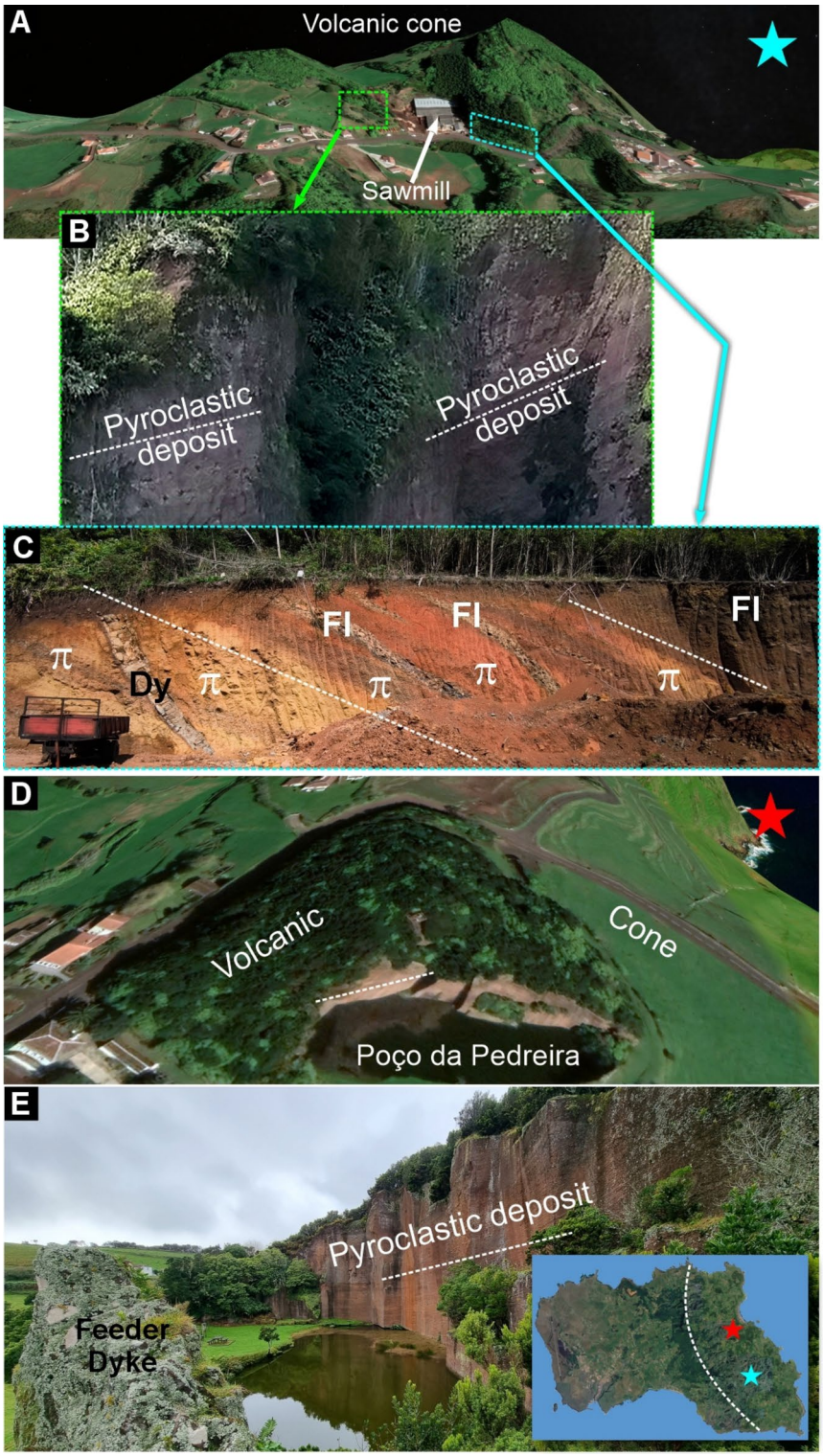

Fig. 5. Two examples of well-exposed volcanic cones in eastern Santa Maria, whose locations are marked by the cyan and red stars on the inset at the bottom right. (**A**) 3-D Google image of the sawmill cone (36° 57′ 34.41″ N; 25° 3′ 0.04″ W). (**B**, **C**) Details of the western (marked by dashed green rectangle in **A**) and eastern (marked by dashed cyan rectangle in **A**) flanks of the cone, respectively showing the expected opposing dips of the flanks (dashed white lines), and other associated structures. *Dy* dyke; *Fl* lava flow; *p* pyroclastic deposit. (**D**) 3-D Google image of the Pico Vermelho cone (36° 58′ 53.55″ N; 25° 3′ 37.52″ W). (**E**) Photograph of the abandoned Poço da Pedreira quarry carved into the western flank pyroclastic deposit.

spotted on the 10 m resolution DEM. Confirmation in the field was carried out by observing the typical volcanic stratigraphy (Fig. 5; pyroclastic layers, with or without intercalated lava flows, all dipping radially to a central crater), sometimes also with outcropping massive necks. We detected ca. 130 cones, of which only 9 occur W of the divide (cf. Fig. S2). 120 cones is the minimum number of cones E of the divide because the terrain is sometimes difficult to access or densely vegetated with no outcrops.

Bathymetry data

Santa Maria lies very close to the junction between the East Azores Fracture Zone (EAFZ), whose scarp is taller than 1000 m, and the Terceira Rift. Important features are observed on the flanks of the island and the surrounding seafloor as depicted in Figs. 6, 7 and 8 and S3: (1) Santa Maria is only conical in the NW quadrant, elsewhere the contours are either straight or concave outwards; (2) the Terceira Rift lies only ca. 25 km east of Santa Maria; (3) south of Santa Maria, the EAFZ is filled with thick sediments; (4) ca. 50 km ESE of Santa Maria, the EAFZ scarp is blanketed by sediments thick enough to completely conceal the EAFZ; (5) these sediments comprise a hummocky terrain with lobes convex outwards (to ESE); (6) a tongue of sinuous sediment lies inside the EAFZ, indicating flow of fine debris into the EAFZ and over an older deposit; (7) SSW of Santa Maria, sediments partially blanket the tall scarp of the EAFZ (Fig. 8 and S5); (8) inside the EAFZ SSW of Santa Maria (Fig. 8 and S6), the thick sediment front is conspicuous (at least 400 m thick; cf. Figure 8), with younger lobes overlying an older and thicker deposit (Fig. 8D); (9) topographic profiles along critical directions show the shape of the topography where we infer the existence (convex upward) or absence (concave upward) of debris deposits (Figs. S4 and S5).

Given that the Terceira Rift (ca. 1.5 to 2 Ma old[37,44,49]) is younger than the Santa Maria's flank collapses (youngest at ca. 3.9 Ma), part of the deposits SE of Santa Maria are currently inside the Terceira Rift, whose bounding fault in the S has displaced the deposits into the rift.

The bathymetry along the seismic reflection profiles is different to the north and east of Santa Maria (Fig. 9A). In the north, the shelf is several kilometres wide, while in the east the slope begins directly at the coast. Along the northern profile 1, and in contrast to the eastern slope, both bathymetry (Fig. 9A) and seismic imagery (Fig. 9B) show parasitic volcanic cones typical of a constructional flank. On the eastern slope of Santa Maria, a channel bends down the slope (Fig. 9C). South of the Formigas High, N-S aligned scarps are present that belong to the western border of the Terceira Rift.

Seismic data

Five seismic units (N1–5) characterize sediments deposited between Santa Maria and Big North seamount (profile 1; Fig. 9B). The internal reflection patterns of Unit N1 are chaotically arranged and are associated with the lower slope of Big North. The subparallel, upward concave reflections of unit N2 overlie unit N1. The reflection amplitudes of unit N2 are still strong on the distal slope, but weaken below units N3-5. Reflection patterns within unit N3 vary from sub-parallel to hummocky. Reflection amplitudes within unit N4 are weak for the most part, though some internal horizons are strongly reflective. Unit N5 shows alternating transparent and strongly reflective layers. Numerous minor faults clearly cut units N4 and N5, but extend down to unit N2 in the north.

Profile 2 (section D-F in Fig. 6B) runs along the shelf with a water depth between 90 and 220 m. No sediment cover is observed. Section E-F crosses the head of the channel that bends down the slope (Fig. 9A). Seismic profile 3, to the ENE of Santa Maria, reveals five seismic units (E1-5). The chaotic reflections within unit E1 are faint. Unit E2 comprises subparallel, downslope diverging reflections. The strong reflections of unit E3 are wavy. The reflection patterns of units E4 and E5 are subparallel, but separated by an unconformity. It is important to note that the seismic data only resolve the upper volcanic units and mass transport deposits. The strong reflection coefficient between hemipelagic sediments and lava or volcaniclastic deposits hampers deeper signal penetration.

We interpret N1/E1 as the volcanic basement of Santa Maria. Reflection patterns like those of N2/E2 have been described by Refs[80,81]. as lava or volcanoclastic sediments. Since N2 superimposes N1 on the slope of Big North, the origin of these deposits is upslope Big North. Unit N3 is a continuation of the lower slope of Santa Maria; its reflection characteristics are similar to lava, an interpretation of seismic data that was confirmed by video surveys on the Azores Plateau[82]. Given that N3 terminates as onlap against N2 from Big North (red half-arrows in Fig. 9B), these lavas are younger than those of Big North. The continuous reflections within N4 and N5 are considered hemipelagic sediments, while we attribute the intercalated transparent layers to mass transport deposits. The undulating reflection patterns of unit E3 resemble those on the northern slope of São Miguel, whose origin was explained as a combination of gravity flow and current impact[83]. We interpret the complex structure of units E4 and E5 as a consequence of tectonics in this section of the Terceira Rift, which formed the N-S directed faults south of the Formigas High (Fig. 9A), and which were described in detail[80]. The undulating depositional patterns on the lower slope of Santa Maria represent levees that are oriented sub-parallel to the channel, and therefore should not be confused with slope-parallel sediment waves that have formed, for example, on the northern slope of São Miguel Island[83]. The upslope source of the turbidity current is not resolved in the data. It is noticeable that, in contrast to the northern flank, no parasitic volcanic cones occur on the eastern flank of Santa Maria. Furthermore, the base of units E2 and E3 is concave upwards.

Numerical modelling

The numerical results for an edifice viscosity of 10^{22} Pa s and a friction angle of 15° (Fig. 10) show that: (1) the island collapses only where there is basal decollement (lefthand side of the edifice), otherwise there is no collapse (righthand side); (2) a main detachment forms where most of the outward motion is accommodated; (3) strain within the collapsing edifice is accommodated by several small synthetic and antithetic faults; (4) when the soft

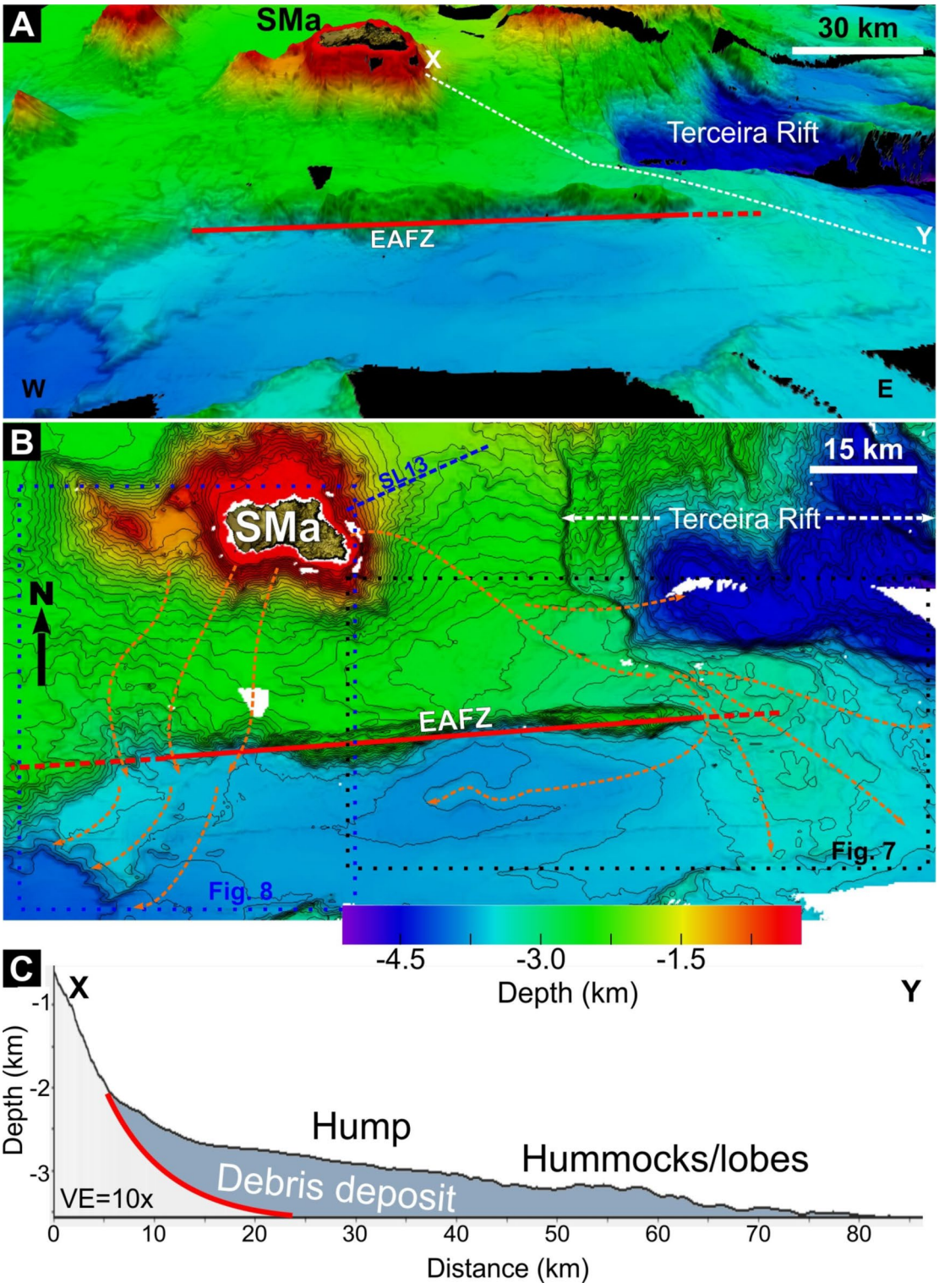

Fig. 6. (**A**) 3-D shaded relief of Santa Maria viewed from the south. Dashed white line marks the position of the topographic profile X-Y shown in (**C**). (**B**) Contoured (100 m) shaded relief with interpreted debris flow lines represented by arrowed orange dashed lines. The red line marks the East Azores Fracture Zone (EAFZ), followed to the east by a dashed red line representing the blanketed EAFZ. Dashed blue line labelled SL13—location of seismic line 13 (see Fig. 9). Dotted black rectangle—location of Fig. 7. Dotted blue rectangle—location of Fig. 8. (**D**) Topographic profile (dashed white line marked X-Y in **A**) showing the upward convex cross-section shape of the debris deposit (hump), including a hummocky/lobed region in the frontal part. Note that after 4 Ma of sedimentation, the size and shape of the blocks/lobes are still recognisable. The red line represents the hypothetical base of the deposit. Multibeam bathymetry from Fig. S1B.

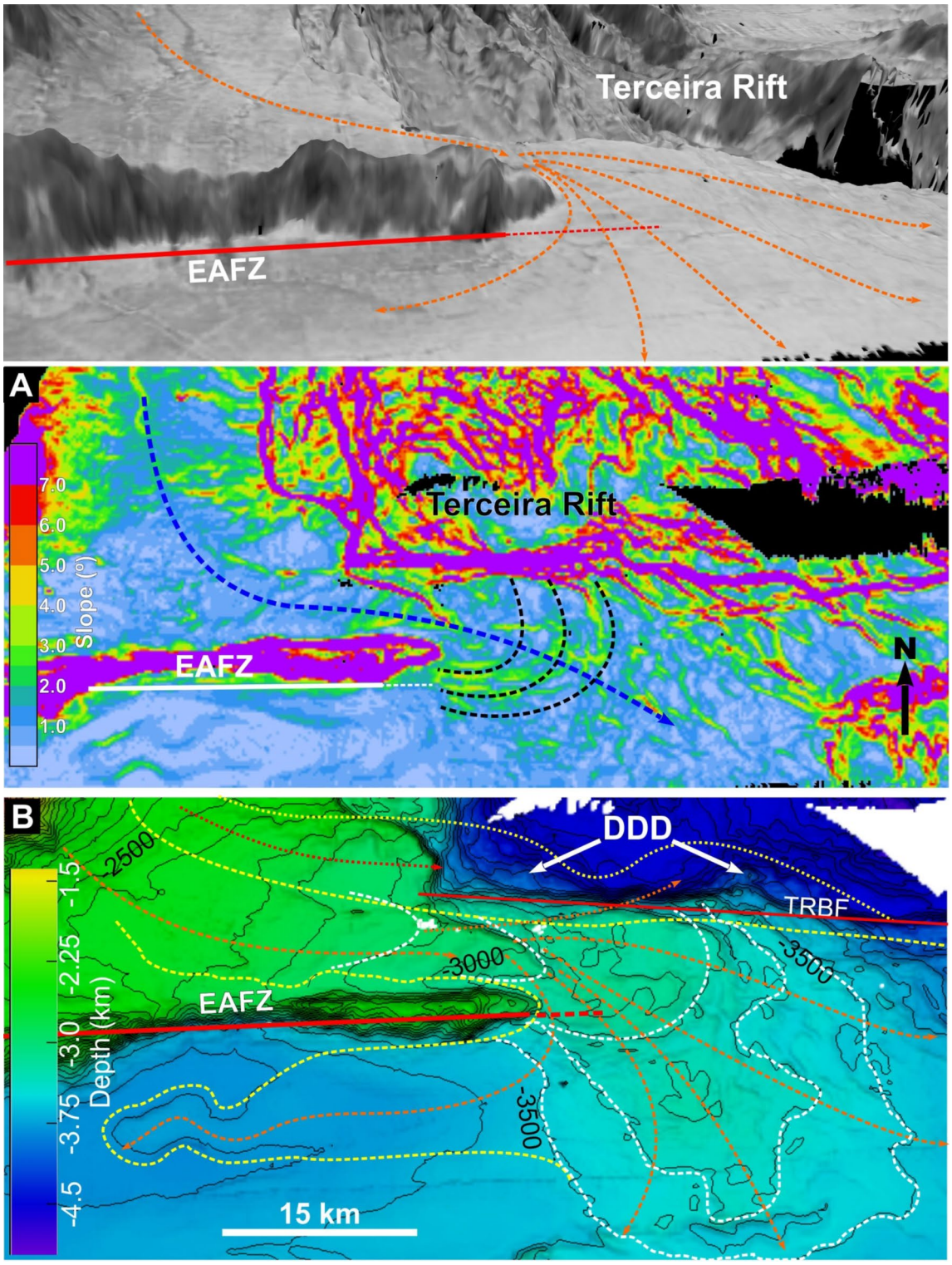

Fig. 7. Images of backscatter, slope and contoured (100 m) shaded relief maps of the sea bottom in the region marked by dotted black rectangle in Fig. 6B. (**A**) Backscatter oblique view from south with interpreted flow lines (dashed orange) on the inferred debris deposit. (**B**) Slope map with lobes interpreted from the curved higher slopes in the region where the EAFZ (red line) scarp is > 1,000 m tall and is blanketed (dashed red line) by the inferred debris deposit. (**C**) Interpreted bathymetry where lobes are outlined by dashed white lines, which we infer to be due to debris flow to the SE (dashed orange arrows). Since the debris deposits should be older than the Terceira Rift, they should be displaced by the main fault bounding the Terceira Rift in the S (red line named TRBF). Two deposits are interpreted inside the Terceira Rift that could correspond to a displaced debris deposit (DDD inside the dotted yellow line). The dashed yellow line delimits the inferred main debris deposit. Note that the slope E of Santa Maria is to the S; therefore, the debris avalanche had to travel to the SE, thus blanketing the EAFZ scarp on the way.

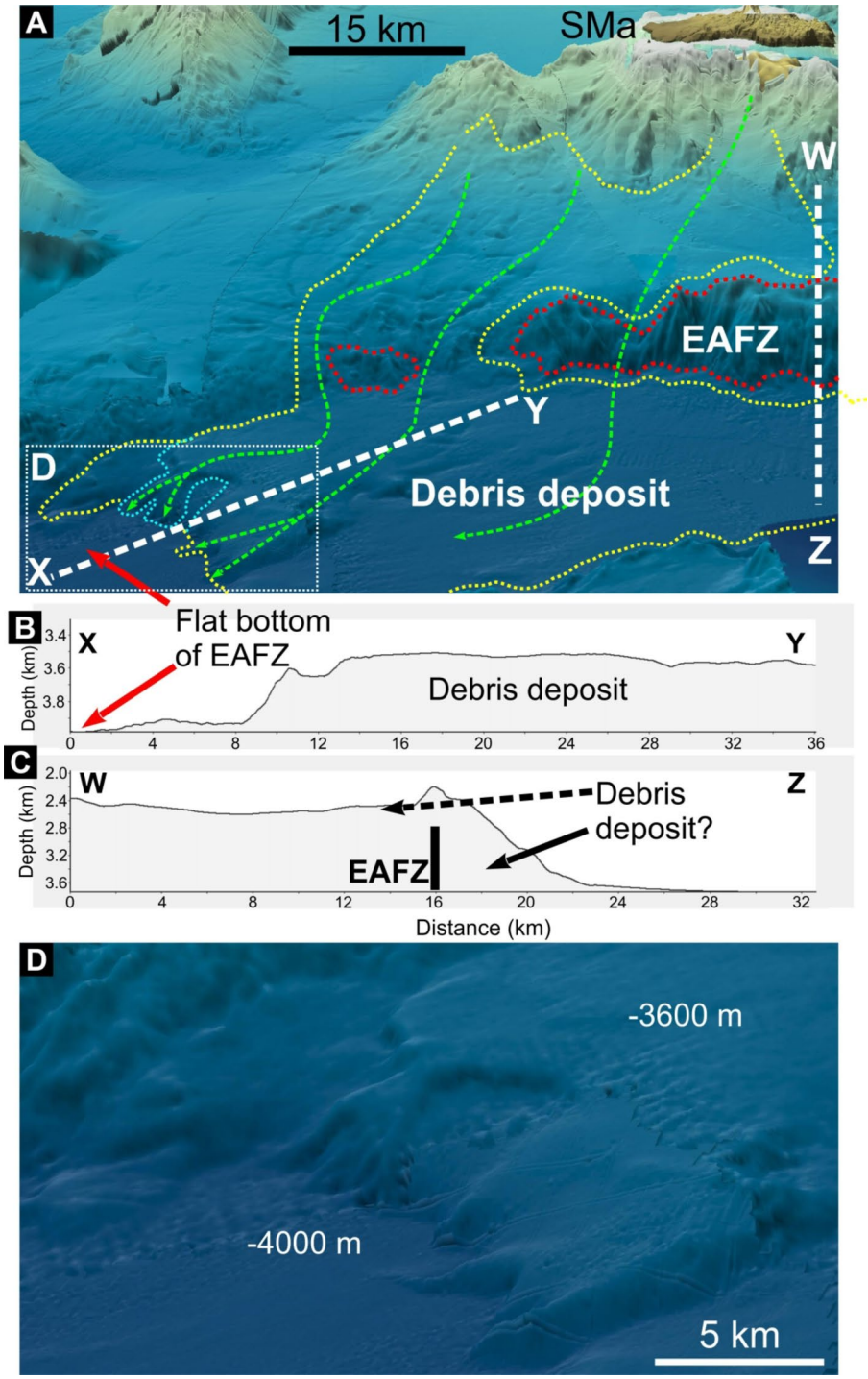

Fig. 8. (**A**) Interpreted shaded relief of SSW Santa Maria (SMa). The red dotted line marks the uncovered scarp of the East Azores Fracture Zone (EAFZ). Green dashed lines represent the flow. The yellow dotted line marks the boundaries of the deposit. The cyan dotted line marks the shape of the younger sediment lobes. (**B**, **C**) Topographic cross-sections showing positions of debris deposits. (**D**) Zoom showing younger lobes on older deposits (marked by the white dotted rectangle in **A**).

layer occupies the whole radius, the entire flank, summit and part of the opposite flank collapse; (5) when the soft layer only partly occupies the base, only partial flank collapse is observed within the relevant time.

Discussion

The possible mechanisms responsible for the vertical motions on Santa Maria Island are diverse. Still, here we will concentrate on two main mechanisms (similar to Ref.[55] for Santiago Island, Cape Verde): top-down

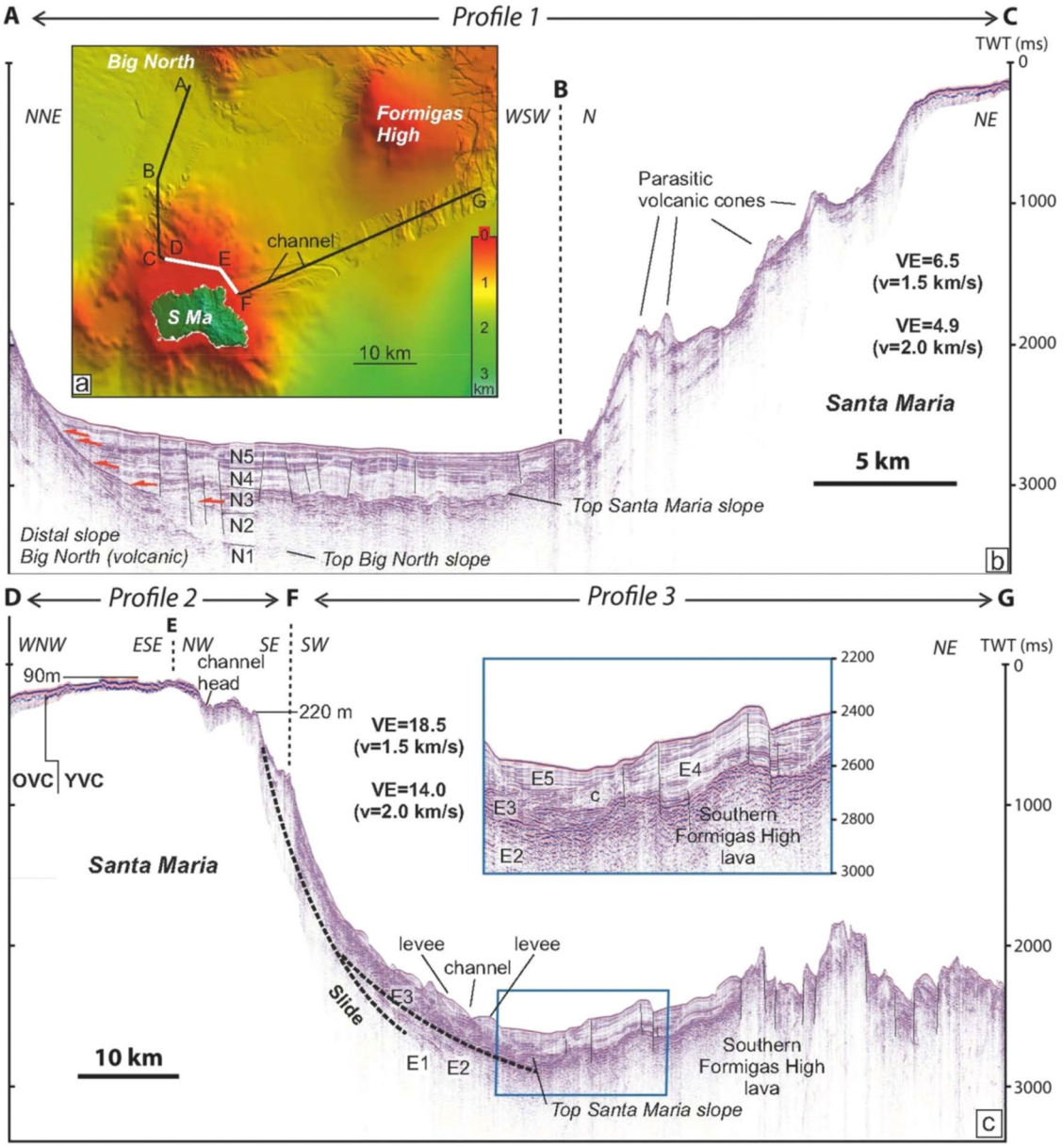

Fig. 9. (**A**) Bathymetry and topography of Santa Maria and adjacent seafloor. High-resolution bathymetry along seismic profiles[67] were plotted above EMODnet data (https://portal.emodnet-bathymetry.eu/). Seamount names Big North and Formigas High according to Ref.[46]. (**B**) Seismic profile HH-P11 from RV Meteor expedition M113/1[68]. N1–5 indicate seismostratigraphic units. (**C**) Seismic profiles HH12-13 from M113/1 expedition. E1–5 indicate seismostratigraphic units.

(island loading and unloading[84]), and bottom-up (lithosphere thinning, underplating, and tectonic uplift), both directly related to isostasy. Before discussing what we think is more relevant to Santa Maria, we must distinguish between the two main processes of vertical movement observed on the island: the older vertical movements due to volcanic construction (subsidence) and collapse destruction (uplift), and the younger vertical movement (uplift) that brought the submarine lavas up to 200 m above current sea level.

Regarding the top-down mechanism, we do not have enough loading/unloading estimates of volumes to justify the inferred subsidence/uplift rigorously. However, we can use the geological observations and well-known equations to assess the effects of volcanic construction (loading) and collapse destruction (unloading) on the vertical movements experienced by Santa Maria. Given that (1) the island currently peaks at 587 m altitude, (2) the inferred collapses removed the summit of the shield volcano, and (3) the submarine Old Volcanic Complex does not outcrop, we can estimate that the original peak altitude was at least close to 1000 m altitude. Therefore, we can use a thickness of 1000 m to calculate the topographic effects of maximum unloading due to the first collapse destruction, and similarly to the loading due to subsequent volcanic construction. We can estimate the isostatic effect of constructional loading by assuming Airy isostasy[85] (i.e., the lithosphere has no strength, and

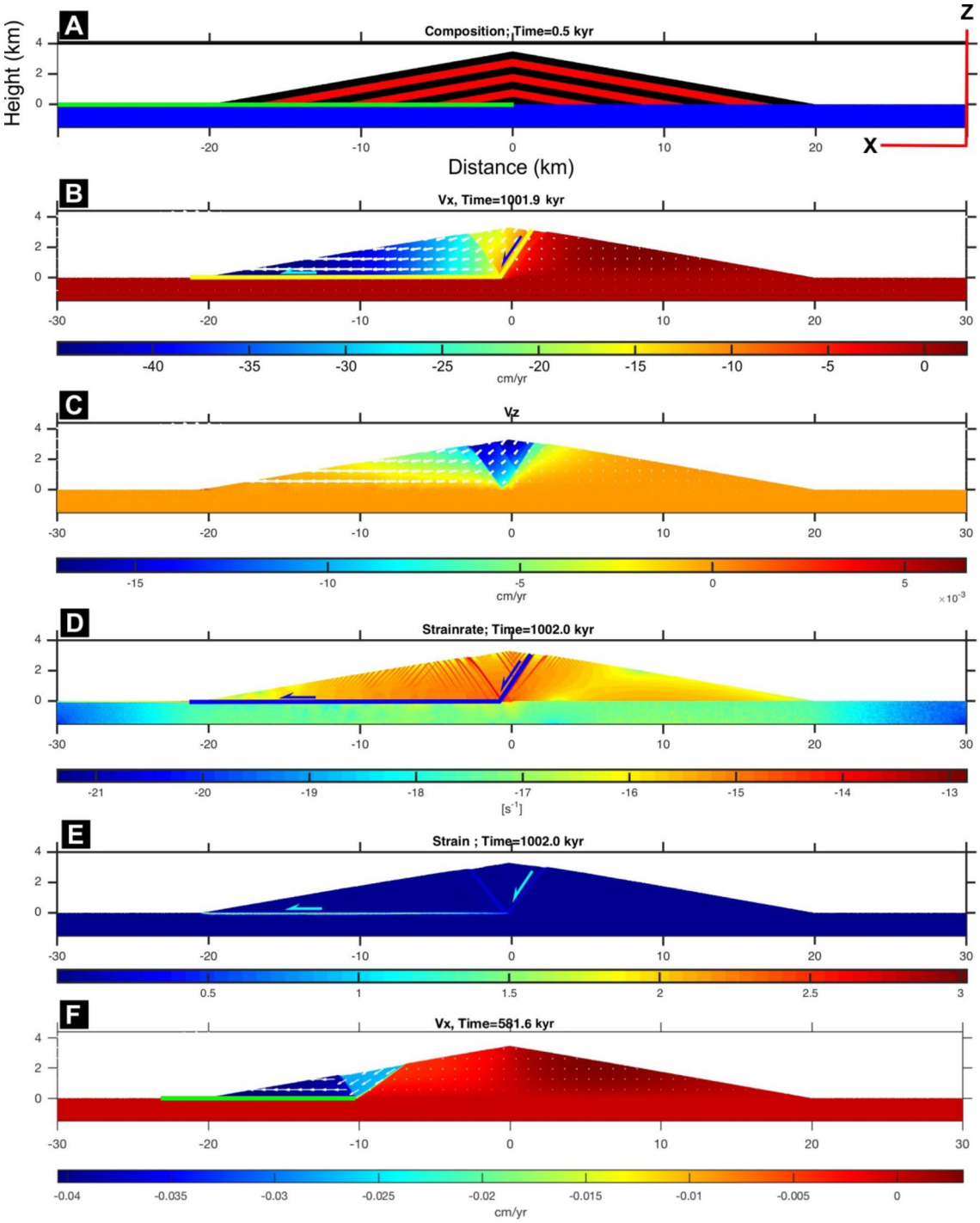

Fig. 10. Model setup and main results. (**A**) Initial model setup for full radius detachment; reference frame on the right-hand side. (**B**,**C**) Velocity maps with the horizontal (Vx) and the vertical (Vz); note that maximum Vz occurs at the volcano's summit, and the maximum Vx lies at the rim of the base. (**D**,**E**) Respectively strain rate and strain maps to show the main faults along which the collapse occurs. (**F**) Partial flank collapse following partial detachment at the base.

the load is locally compensated) and a maximum 1000 m thickness of the Old Volcanic Complex and Young Volcanic Complex: $h = e - (e * \rho l/\rho a) = 1000 - (1000 * \rho l/\rho a) = 1000 - (1000 * 2800/3300) = 1000 - 849 = 150$ m, where h is the vertical displacement (m), e is the thickness of the added/removed material (m), ρl is the density of the lavas (kg/m^3), and ρa is the density of the asthenosphere (kg/m^3). 150 m is our conservative estimate of the isostatic response to constructional/destructional loading/unloading, which is within the range of altitudes observed in SW Santa Maria (cf. Figure 4).

Given that the second major collapse was followed by volcanic construction (loading = subsidence), we cannot use the above calculations to explain the submarine lavas currently outcropping up to 200 m altitude. Therefore, an alternative explanation must be sought. Different bottom-up mechanisms can be responsible for the inferred vertical movements (up to 200 m): thinning of the lithosphere by basal erosion, or crustal underplating[50,86], or the arrival of a thermal mantle plume, or tectonic uplift. Reference[55] performed 1-D numerical simulations solving the heat transport equation to calculate the uplift resulting from density variations. They concluded that all mechanisms could account for the vertical movements observed on Santiago Island, Cape Verde. The calculations can be directly extrapolated to Santa Maria, but the discussion of the most probable mechanism must be different because the tectonic settings are very different: within-plate, thermal mantle plume-related volcanism (Cape Verde) in contrast to rift-related volcanism (Santa Maria). While Ref[55]. suggested magma underplating to explain the young uplift of Santiago Island (submarine lavas currently up to 400 m altitude), and Ref.[50] proposed magma underplating for Santa Maria, here we cannot use this explanation because the island sits on the western shoulder of the Terceira Rift, thus being subject to the effects of rift shoulder uplift since at least 1.5 Ma, the age estimated for the Terceira Rift[37,44,49]. We are not excluding magma underplating as a viable mechanism for Santa Maria, we argue that rift shoulder uplift cannot be ignored because it is geological evidence that can explain the observed uplift by itself.

Volcanic ocean islands can be significantly modified by erosion between periods of volcanic construction, the critical question being what kind of erosion. Two typical kinds of erosion are meteoric and marine erosion (long-term), and gravitational failure (large-scale landsliding–short-term). If one chooses to explain the destruction of most of the original two shield volcanoes, especially the older one in Santa Maria, by marine and meteoric erosion, then one must explain three main observations: (1) erosion leads to loss of mass and consequent isostatic uplift, which is the opposite of what is observed. (2) The last 3 Ma were not enough to significantly destroy the island, and not even the ca. 3.6 Ma Strombolian cones as well illustrated in Fig. 4. Therefore, 0.2 Ma should not be enough to remove the missing eastern flank, the summit and part of the western flank of the older volcano. (3) The dominant and strong winds blow from SW and NW, therefore they cannot justify the much greater erosion in eastern Santa Maria. All they can justify is the wider marine shelf observed in the north. Smaller landslides have removed appreciable pieces of the island in the south and west[38], thus justifying the narrower shelf, despite the favourable orientation for greater marine erosion by the strong winds.

The possible relations between a main subaerial volcano and parasitic cones are illustrated in Fig. 11 for the cases of absence (Fig. 11A) or presence of flank collapses (Fig. 11B–D). Conformable parasitic cones sitting on the convex surface of a shield volcano should be the most common case (Fig. 11A). However, this is not what we observe on the eastern flanks of both old and new main shield volcanoes. The new shield volcano (Young Volcanic Complex) grew on the collapse scar of the old shield volcano (Old Volcanic Complex), and the young shield volcano shows few Strombolian cones on the convex surface (conformable) and many Strombolian cones on the concave surface (unconformable). If there had been no collapse, all parasitic cones would lie on a conical surface convex outward, which is not the case. Looking at the current topography east of the divide (Fig. 3A), one might get the impression that the eastward concave surface is the result of recent meteoric erosion. However, this is not the case because this concave surface is covered with more than one hundred Strombolian cones with ages around 3.6 Ma. This means that the surface where they sit must be older than 3.6 Ma, but not older than 4.0, the age of the lava flows that comprise the basement of the Strombolian cones. These have well survived 3.6 Ma of meteoric erosion, thus preserving the shape of the concave surface where they grew. The concave surface seems to result from erosion, the problem being what kind of erosion. A 0.2 Ma lag between volcanic construction and destruction is not enough for meteoric erosion to remove more than half of the young shield volcano; in fact, not even 3.6 Ma have been enough for meteoric erosion to remove the Strombolian cones. Therefore, the conspicuous concave shape of eastern Santa Maria is not an erosional feature younger than 3 Ma, it is a scar of a full-flank sector collapse that took place ca. 3.9 Ma ago (Fig. 11C, D) fossilised by the many parasitic cones that grew between 3.6 and 2.8 Ma. The great number of Strombolian cones on the eastern concave surface of Santa Maria lie on the wrong surface (unconformity), because they should lie on a convex surface of a typical volcanic shield if there had been no collapse (Fig. 11A). The many Strombolian cones are responsible for the partial filling of the collapse scar; therefore, the original scar is not so prominent on the bathymetry. We note that the eruptive style changed from a dominant shield volcano to numerous asymmetrically distributed Strombolian cones that grew unconformable on the eastern concave scarp facing east, at around 3.6 Ma. This contrasting volcanic style change is an additional indication that erosion was by a collapse, most likely a full-flank sector collapse that affected the deep volcanic plumbing system to the point of changing the eruptive style.

Regarding the bathymetry, we recall two critical features ESE of Santa Maria that robustly support our interpretation of debris avalanche deposit: (1) the complete blanketing of the prominent (ca. 1000 m tall) East Azores Fracture Zone ca. 50 km SE of Santa Maria, which we interpret as blanketing by a debris avalanche deposit; (2) the curved (convex to the SE) lobes indicating the sense of flow, which we also interpret as the product of a debris avalanche deposit running down the ESE slope of Santa Maria. Some alternative explanations to these critical observations on the bathymetry can be envisaged: (1) Lava flow—this is unlikely because it would have to be a single flow, since the lobes can be found in individual lava flows, and the lava flow would have to be bigger than the island itself (cf. Fig. 9); (2) pelagic sediments—again, the dimensions are too big, especially the thickness, as shown by the thickness of pelagic sediments in the seismic profile; (3) pyroclastic flow—Santa Maria is basaltic, and no signs of Plinian volcanic activity have ever been observed on the island or nearby, so this hypothesis can be ruled out. We conclude, therefore, that the most plausible explanation is debris avalanche deposit. We show with topographic profiles (Figs. S4, S5) that the topography is convex downwards in the absence of debris deposits, and convex upwards when cutting across debris deposits, thus reflecting the accumulation of excessive debris/sediments (as done in Hawaii[2]).

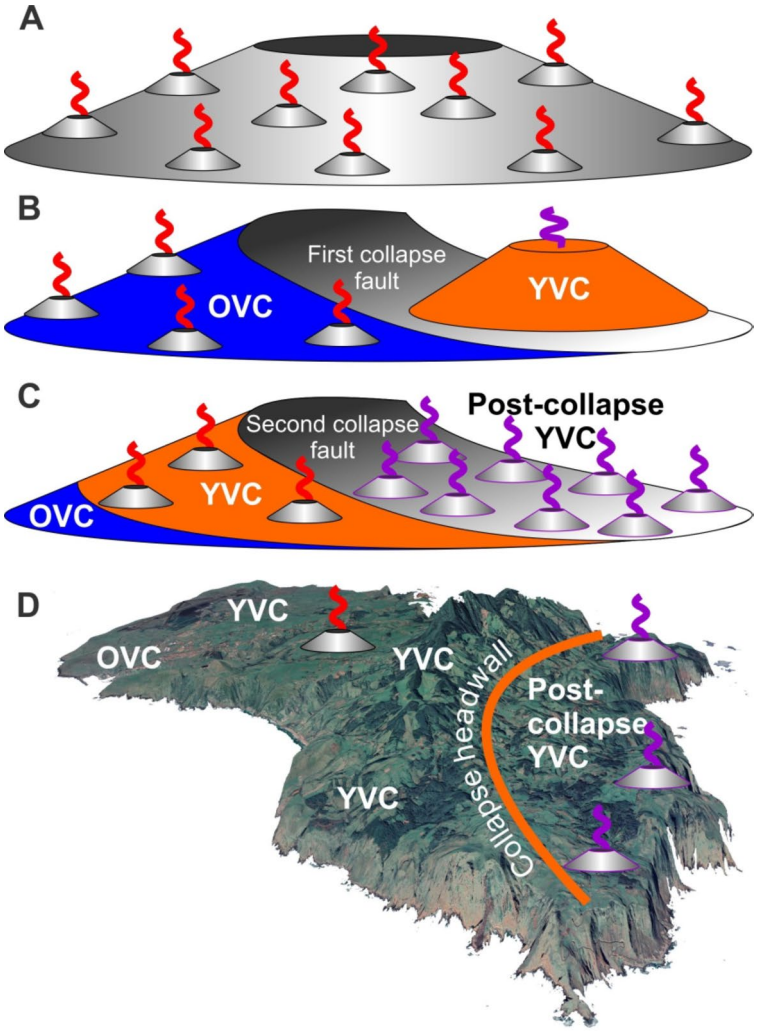

Fig. 11. Sketches to illustrate the possible relations between a main subaerial volcano and parasitic cones in the cases of absence (**A**) or presence of flank collapse (**B–D**). (**A**) Conformable parasitic cones sitting on the convex surface of a shield volcano is the most common case. (**B**) Collapsed old shield volcano (OVC) with new shield volcano (YVC) growing on the collapse scar. (**C**) Young shield volcano with few Strombolian cones on the convex surface (conformable), and many Strombolian cones on the concave surface (unconformable). (**D**) 3-D shaded relief of Santa Maria viewed from SE showing the position of the main volcanic complexes, the scar of the collapse headwall, and the conformable (cones with red sinusoid) and unconformable (cones with purple sinusoid) parasitic cones.

Regarding the available seismic profile, we must bear in mind that it does not cross the inferred debris avalanche deposit; at best it crosses the uppermost portion of the deposit because the slope east of the island is quite steep to the S and ESE. If it is correct that all we see below the well-stratified sediments are lava flows close to the Santa Maria edifice, then we do not see the underlying inferred debris-avalanche deposit, which is consistent with the onshore observations and interpretations: shield volcano, collapse (debris deposit), renewed volcanism by Strombolian cones filling the scar, and finally extinction of volcanism and normal ocean bottom sedimentation (pelagic and from island erosion).

Observations of hydroacoustic and seismic data show two contrasting slopes in the Santa Maria edifice: (1) a constructive northern slope with volcanic cones, whose base mimics the base of an originally conical Santa Maria edifice; and (2) a fairly straight and north-south trending, upward concave slope that has been cleared of volcanic cones. Similar observations were made at the D. João de Castro seamount in the Hirondelle Basin[87], the Terceira Rift segment NW of São Miguel Island. There, seismic and bathymetric data show that the flanks in some segments have been swept bare by landslides. The parasitic volcanic cones were destabilized and remobilized together with the slope sediments. These geophysical observations allow the conclusion that the east slope of Santa Maria has collapsed.

To estimate the volumes of the two collapses, we use the procedure reported by Ref.[88]: we approximate the shape of the collapse to a spherical cap because the collapse fault is curved along both dip and strike. Then we calculate the volume of a spherical cap assuming values of the radius of the approximated circumference (ca.

7 km, measured as shown on the sketch in Fig. S7) and the height of the spherical cap (ca. 1.4 km), and we obtain ca. 110 km^3 for each of the collapses. The volume of the volcanic edifice is estimated at ca. 1.26×10^3 km^3, considering a simple conical geometry with 20 km radius and 3 km height; such volume may actually be a maximal value as volcanic islands are not idealized regular cones, but typically display lower slopes in the sub-aerial domain[64]. Therefore, we infer that more than 10% of the edifice collapsed in each event. The estimated Santa Maria volume is ca. 170 times smaller than the volume estimated for the Big Island in Hawaii (about 213,000 km^3; Ref.[89]), which can be used as an argument to claim that small islands like Santa Maria do not have enough mass to undergo full-flank sector collapses.

We did not attempt to estimate the volume of the debris deposits on the ocean floor because: (1) the original topography is complex; (2) the aerial extent cannot be reasonably assessed because the debris deposits of both Santa Maria collapses predate the opening of the Terceira Rift, which means that they are affected by the opening of the new rift and, therefore, the deposits were larger than they currently seem at a first glance; (3) the thickness and composition are inaccessible in the absence of seismic soundings; and (4) the volume of entrained sediments into the avalanche can be very large[90] and is not known. From the great aerial extent of the debris deposits, we infer a large entrainment of sediments deposited earlier (in the previous 30 Ma).

Analogue and numerical modelling of giant flank collapses affecting volcanic islands has concentrated on relatively large edifices (e.g. Hawaii), and has mostly considered a full detachment of the volcano's base[6,7,91–93]. However, Ref[8]. tested experimentally the effects of a weak substrate (silicone putty) with different shapes and extent relative to the radius of the base of the volcanic (sand) cone. In terms of mechanics, one cannot model the behaviour of a full volcano edifice using basalt rheology, because volcanic edifices are known to be weak and basalt is very strong. Typical basaltic volcanic edifices are made of alternating pyroclastic deposits (mechanically very weak) and lava flows pervasively fractured (also mechanically weak at the macroscale). Additionally, lava flows contact with one another through irregular and non-cohesive surfaces; therefore, volcanic edifices are weak as a whole, not as strong as a pristine basalt at the scale of millimetres or centimetres. These characteristics make volcanic edifices yield by spreading and brittle failure, and that is why we used viscoplastic rheology to obtain simultaneous spreading and faulting in the models. For a more complete rationale of using a viscous rheology to simulate the volcanic edifice, we refer the reader to Ref[7].

The present numerical simulations indicate that: (1) partial basal detachment produces partial flank collapses, like the Hilina Slump in the Big Island, Hawaii. From this, we infer that the pressure and temperature induced by the Hawaiian edifice transformed the soft sediment into strong rock hampering full detachment at the volcano's base. (2) To have a full-flank sector collapse (i.e. full flank and summit), like in Santa Maria, a full radius at the volcano's base must detach, similarly to the analogue modelling of Ref.[8] and the numerical simulations reported here. From this, we conclude that the pressure and temperature induced by the Santa Maria edifice could not transform the soft sediment into strong rock that could hamper full detachment and, thus, the inferred full-flank sector collapse. (3) A viscosity in the order of 10^{23} Pa s prevents collapse in relevant time, and a viscosity in the order of 10^{21} Pa s makes the volcanic edifice rapidly collapse into a flat pancake. From this and the gathered natural data, we infer that a viscosity in the order of 10^{22} Pa s realistically approximates the behaviour of a volcanic edifice like Santa Maria. We could make collapse velocities more similar to nature by lowering the viscosity a bit, but a full parameter investigation and sensitivity analysis are out of the scope of this study.

Given Santa Maria's sediment substrate and the results of the present numerical modelling, we infer that the dominant instability factor was basal detachment along a weak substrate. The Santa Maria volcanic edifice does not have steep flanks (< 10° on average), therefore the effect of slope magnitude is not considered here. The weak substrate inferred as the main instability factor in Santa Maria could apply to all volcanic ocean islands that are significantly younger than the underlying oceanic crust where soft sediments cover the magmatic crust.

A volcanic edifice can spread under its own weight, especially if it sits on a weak substrate, but it can do so slowly as a slump (e.g. the Hilina Slump in the Big Island, Hawaii[4,94,95]). The new bathymetry indicates that the collapse was catastrophic at some point because the debris travelled far from the source (at least 100 km, i.e. more than two times the radius of the Santa Maria edifice at the base). The switch from slow slump to fast catastrophic collapse may have been triggered by high-magnitude earthquakes in the nearby East Azores Fracture Zone, which was the active Nubia-Eurasia plate boundary during Santa Maria's volcanic lifetime. Note that the inferred flank collapses in Santa Maria pre-date the jump of the Nubia-Eurasia plate boundary from the East Azores Fracture Zone to the Terceira Rift around 1.5 to 2.0 Ma[37,44,49]. The collapses apparently occurred to the east (mostly) and the south, and this could be due to the topography underlying Santa Maria. The absence (at least not yet observed) of westwards collapses can be due to the buttressing offered by the submarine volcanic ridge lying west of Santa Maria.

Conclusions

Santa Maria's story is made up of downs and ups, as a response to episodes of volcanic construction (down) and massive collapse destruction (up), respectively. Early volcanic construction makes an edifice go down (lithospheric bending by loading) (Fig. 12A), and continued volcanism brings the volcanic edifice from a seamount to an island—the first island (Fig. 12B). In Santa Maria, this happened at ca. 6 Ma. Subsequent destruction by a full sector collapse to the seafloor away from the island's base has the opposite effect, i.e. the edifice goes up because the elastic lithosphere is partially unloaded and unbends (Fig. 12C). This happened in Santa Maria at ca. 5.1 Ma following the first sector collapse. A subsequent construction phase, starting with a new submarine volcano growing on the scar of the first collapse, again loads and bends the lithosphere downward (second subsidence), and the emergence of the second volcano gives birth to a new island—the second island (Fig. 12D). This took place in Santa Maria between ca. 4.9 and 3.9 Ma. A second collapse again unloads the lithosphere (uplift; Fig. 12E), and subsequent constructional volcanism again loads the lithosphere (subsidence). This second collapse occurred in Santa Maria at ca. 3.8 Ma (Fig. 12E) and new volcanism comprising hundreds

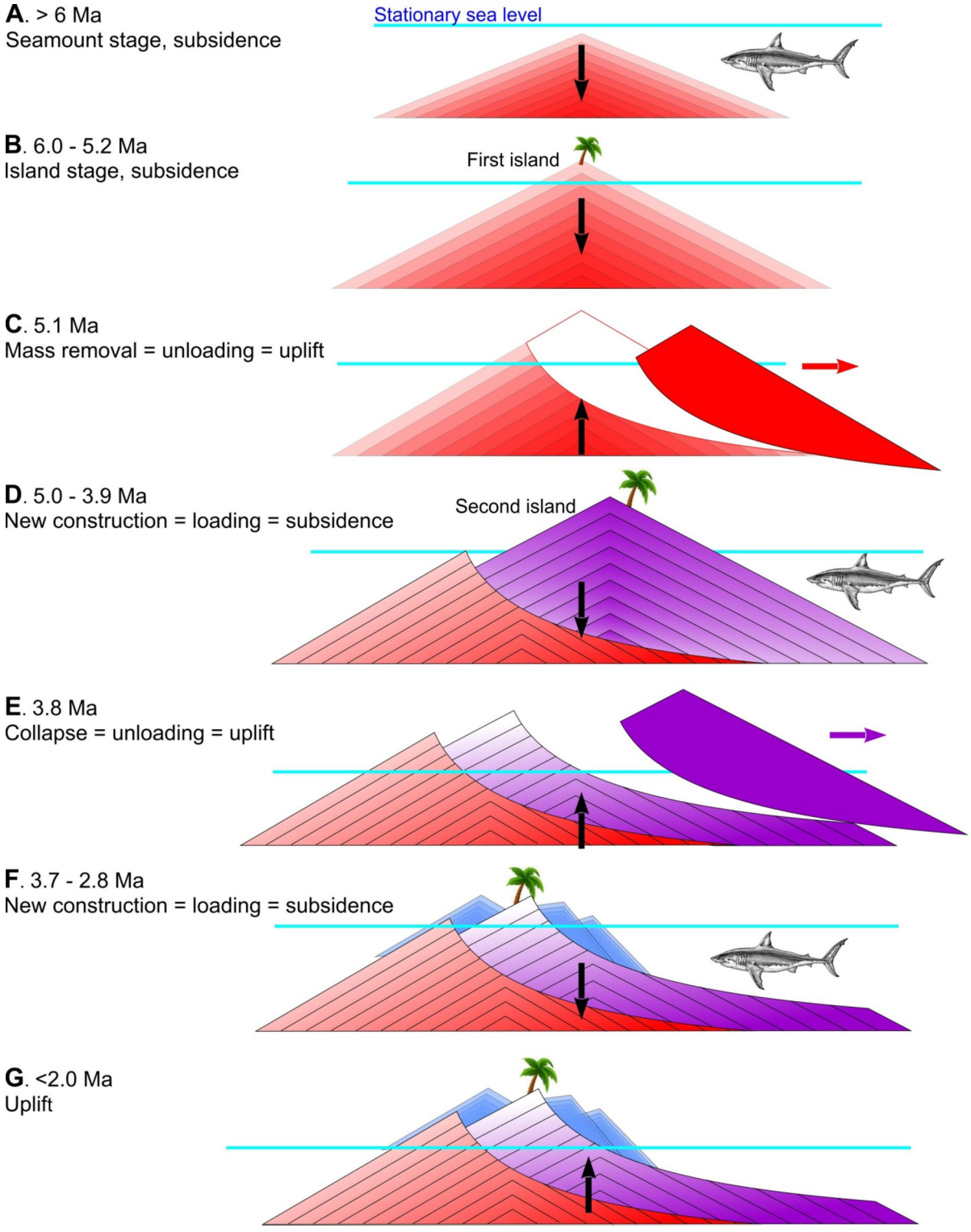

Fig. 12. Cartoon illustrating the complex evolution of a volcanic ocean island like Santa Maria Island in the Azores, highlighting the successive episodes of volcanic construction and collapse destruction responsible for subsidence and uplift, respectively, due to loading and unloading of the elastic lithosphere.

of Strombolian cones followed until ca. 2.8 Ma ago (Fig. 12F). More recent uplift (Fig. 12G) can be explained in different ways: by underplating[50] or by Terceira Rift shoulder uplift after ca. 2 Ma[38].

Several problems are outlined in the Introduction section, and the following are our explanations based on fieldwork, geochronology, and marine geophysical data. Santa Maria Island has been destroyed appreciably by marine erosion in the north, where the island has not undergone more recent medium-sized collapses. The

good preservation of the Strombolian cones for more than 3 Ma attests to the less destructive effects of meteoric erosion onshore. If the island is still mostly preserved after ca. 3 Ma, we cannot see how it could have been massively destroyed in a couple of hundreds of years by meteoric and marine erosion in the past. We infer that two full sector collapses removed the summits and the eastern flanks of the two main volcanoes at ca. 5.1 and 3.8 Ma to explain that lava flows always dip to the west, except close to the sea on the eastern coast. The eastern coast lies inside the scar of the youngest collapse, where the Strombolian cones developed and whose lavas flowed to the sea in the east (Fig. 12F).

Current knowledge on sea level change cannot explain the shift from subaerial to submarine volcanism at ca. 5 Ma. Our best explanation is isostasy by loading and unloading cycles bending and unbending the lithosphere. The observation that only a few Strombolian cones exist on Santa Maria's western flank and more than one hundred exist on the eastern flank can be explained by a change in volcanic style from main shield volcano to more than one hundred Strombolian cones at ca. 3.9 Ma. We infer that the second collapse disturbed the deep volcanic plumbing systems, thus producing a different volcanic style. The western flank of the main volcano does not seem to have been affected by any major collapse, therefore the plumbing system was kept intact, and the few cones standing conformably on the western flank are no more than common adventitious cones. The nature and age of the conspicuous eastward concave topography in eastern Santa Maria cannot be due to marine and meteoric erosion as concluded above, and cannot be younger than ca. 3.4–3.6 Ma because this is the age of the volcanic cones sitting on the concave topography. Given that this shape is the opposite of a cone, and lava flows dip to the west, we conclude that the concave surface represents the scar of a full sector collapse. The sediments underlying Santa Maria can be responsible for the inferred large-scale mass wasting because the volcanic edifice can spread on them, thus leading to failure by full sector collapse if the whole base is weak, as indicated by the numerical simulations. The new marine geophysical data support our interpretations inferred from onshore data.

With the new high-resolution bathymetry, we found that the missing flanks are deposited at the bottom of the ocean, which supports the onshore data and earlier interpretations, and better helps to estimate the dynamics of the debris avalanches (runout distance, flow, area covered by slide deposits, size of debris, type of collapse—slow or catastrophic). Previous onshore and new bathymetric data on and around Santa Maria Island concur toward the same conclusion: the island has experienced two major flank collapses, the debris of which lie on the ocean floor south and southeast of the island. Given that the collapses occurred some millions of years ago, it is difficult to discern between the deposits resulting from the two collapses. However, from the distance travelled by large blocks and the volume of entrained sediments (at least 100 km away from an island that is < 20 km wide), we infer that both collapses were catastrophic. Since Santa Maria lies very close to the East Azores Fracture Zone (only a few km apart), which was active at the time of the collapses, the catastrophic collapses may have been triggered by shallow earthquakes occurring nearby in the East Azores Fracture Zone.

We estimated the isostatic effect of constructional loading and destruction unloading by assuming Airy isostasy, and found a conservative value of ca. 150 m for the amplitude of vertical movements. This estimate and the consistency with geological observation indicate that loading/unloading processes can account for the inferred vertical movements before ca. 3.1 Ma and were responsible for the observed alternation between subaerial and submarine lavas.

The numerical simulations presented here are consistent with the analogue experiments of Ref.[8], and indicate that, if the volcanic edifice is strong, it does not collapse, even if its base is weak. However, a relatively weak edifice can collapse over a weak base. We conclude that small volcanic islands can collapse when both the edifice and its base are weak. From the numerical results, we infer that Santa Maria's edifice is not hot and big enough to induce pressure/temperature conditions that could transform soft sediment into hard metamorphic rock, thus hampering collapse. This weak layer can promote detachment at the base, which facilitates deep flank collapses as indicated by the missing flank, the volume of the ocean bottom debris deposits, and the numerical simulations presented here. This would explain why the Azores (small islands) and Canary Islands (bigger but still relatively small) show so many large-scale flank collapses and ongoing slumps: they both sit on soft sediment. Our numerical simulations also indicate that, if the basal detachment only partially occupies the base of the volcano edifice (outer soft sediment ring less affected by pressure and temperature), the flank will only partially collapse, which does not seem to be the case in Santa Maria. This could be the case of the Hilina Slump in the Big Island of Hawaii because the large size of the edifice can produce high-grade metamorphism in the sediments at the core of the edifice's base.

Confirmation that the collapses have occurred increases both hazard and risk, because the number of recognised collapses increases, and so does the frequency, thus bringing closer the time scales of collapses and human life.

Data availability

The bathymetric data that support the findings of this study are available from the Task Group for the Extension of the Continental Shelf (EMEPC) but restrictions apply to the availability of these data, which were used under license for the current study, and so are not publicly available. Data are however available from the authors upon reasonable request to Luísa Pinto Ribeiro (luisa.ribeiro@emepc.mm.gov.pt) and with permission of the EMEPC. Supplementary datasets generated and/or analysed during the current study are available on the EMODnet repository at https://portal.emodnet-bathymetry.eu/?menu=19. The joint Meteor MB data are available upon request to Christian Hübscher (Christian.Huebscher@uni-hamburg.de) and from PANGAEA[67]. Bathymetric data shown in Fig. 1 can be downloaded from Hübscher and Beier[67]. Seismic reflection data can be found on ZENODO database[96].

Received: 17 September 2024; Accepted: 16 January 2025
Published online: 30 January 2025

References

1. Moore, G. J. Giant submarine landslides on the Hawaiian Ridge. *U. S. Geol. Surv. Prof. Pap.* **501-D**, D95–D98 (1964).
2. Moore, J. G. et al. Prodigious submarine landslides on the Hawaiian Ridge. *J. Geophys. Res.* **94** (465–17), 484 (1989).
3. Moore, J. G. & Moore, G. W. Deposit from a giant wave on the island of Lanai, Hawaii. *Science* **226**, 1312–1315 (1984).
4. Moore, J. G., Normark, W. R. & Holcomb, R. T. Giant hawaiian landslides. *Annu. Rev. Earth Planet. Sci.* **22**, 119–144 (1994).
5. Siebert, L. Large volcanic debris avalanches: characteristics of source areas, deposits, and associated eruptions. *J. Volc. Geotherm. Res.* **22**, 163–197 (1984).
6. Borgia, A., Ferrari, L. & Pasquarè, G. Importance of gravitational spreading in the tectonic and volcanic evolution of Mount Etna. *Nature* **357**, 231–235 (1992).
7. Borgia, A. The dynamic basis of volcanic spreading. *J. Geophys. Res.* **99**, 17791–17804 (1994).
8. Andrade, S. D. & van Wyk de Vries, B. Structural analysis of the early stages of catastrophic stratovolcano flank-collapse using analogue models. *Bull. Volcanol.* **72**, 771–789 (2010).
9. Norini, G. & Acocella, V. Analogue modelling of flank instability at Mount Etna: understanding the driving factors. *J. Geophys. Res.* **116**, B07206 (2011).
10. Murray, J. B., van Wyk de Vries, B., Pitty, A., Sargent, P. & Woller, L. Gravitational sliding of the Mt. Etna massif along a sloping basement. *Bull. Volc.* **80**, 40 (2018).
11. Voight, B. & Elsworth, D. Failure of volcano slopes. *Geotechnique* **47**, 1–31 (1997).
12. Elsworth, D. & Day, S. J. Flank collapse triggered by intrusion: the canarian and Cape Verde archipelagos. *J. Volc. Geotherm. Res.* **94**, 323–340 (1999).
13. Hürlimann, M., Garcia-Piera, J. O. & Ledesma, A. Causes and mobility of large volcanic landslides: application to Tenerife, Canary Islands. *J. Volc. Geotherm. Res.* **103**, 121–134 (2000).
14. Hürlimann, M., Turon, E. & Martí, J. Large landslides triggered by caldera collapse events in Tenerife, Canary Islands. *Phys. Chem. Earth (A)* **24**, 921–924 (1999).
15. Krastel, S. et al. Submarine landslides around the Canary Islands. *J. Geophys. Res.* **106**, 3977–3997 (2001).
16. Rincon, M. et al. Contrasting catastrophic eruptions predicted by different intrusion and collapse scenarios. *Sci. Rep.* **8**, 6178 (2018).
17. McGuire, W. J. Volcano instability: a review of contemporary themes. *Geol. Soc. Lond. Spl. Publ.* **110**, 1–23 (1996).
18. Norini, G. et al. Large scale landslides triggered by quaternary tectonics in the Acambay Graben, Mexico. *Earth Surf. Process. Land.* **35**, 1445–1455 (2010).
19. Wang, J., Ward, S. N. & Xiao, L. Tsunami squares modeling of landslide generated impulsive waves and its application to the 1792 Unzen-Mayuyama megaslide in Japan. *Eng. Geol.* **256**, 121–137 (2019).
20. Reid, M. E., Sisson, T. W. & Brien, D. L. Volcano collapse promoted by hydrothermal alteration and edifice shape, Mount Rainier. *Wash. Geol.* **29**, 779–782 (2001).
21. Norini, G. et al. Unusual volcanic instability and sector collapse configuration at Chimpa volcano, central Andes. *J. Volc. Geotherm. Res.* **393**, 106808 (2020).
22. Hevia-Cruz, F. et al. Weathering pulses during glacial-interglacial transitions: insights from well-dated paleosols in the Azores volcanic province (Central North Atlantic). *Q. Sci. Rev.* **324**, 108438 (2024).
23. Day, S. J. Hydrothermal pore fluid pressure and the stability of porous, permeable volcanoes. *Geol. Soc. Lond. Spl. Publ.* **110**, 77–93 (1996).
24. Heap, M. J., Farquharson, J. I., Wadsworth, F. B., Kolzenburg, S. & Russell, J. K. Timescales for permeability reduction and strength recovery in densifying magma. *Earth Planet. Sci. Lett.* **365**, 212–222 (2013).
25. Masson, D. G., Harbitz, C. B., Wynn, R. B., Pedersen, G. & Løvholt, F. Submarine landslides: processes, triggers and hazard prediction. *Philos. Trans. R. Soc. Math. Phys. Eng. Sci.* **364**, 2009–2039 (2002).
26. Crosta, G. B. & Dal Negro, P. Observations and modelling of soil slip-debris flow initiation processes in pyroclastic deposits: the Sarno 1998 event. *Nat. Hazards Earth Syst. Sci.* **3**, 53–69 (2003).
27. Quidelleur, X., Hildenbrand, A. & Samper, A. Causal link between quaternary paleoclimatic changes and volcanic islands evolution. *Geophys. Res. Lett.* **35**, L02303 (2008).
28. Boulesteix, T., Hildenbrand, A., Soler, V., Quidelleur, X. & Gillot, P. Y. Coeval giant landslides in the Canary Islands: implications for global, regional and local triggers of giant flank collapses on oceanic volcanoes. *J. Volc. Geotherm. Res.* **257**, 90–98 (2013).
29. Clare, M. A. et al. Complex and cascading triggering of submarine landslides and turbidity currents at volcanic islands revealed from integration of high-resolution onshore and offshore surveys. *Front. Earth Sci.* **6**, 223 (2018).
30. Mitchell, N. C. Susceptibility of mid-ocean ridge volcanic islands and seamounts to large-scale landsliding. *J. Geophys. Res.* **108**, 2397 (2003).
31. Woodhall, D. Geology and volcanic history of Pico Island Volcano, Azores. *Nature* **248**, 663–665 (1974).
32. Hildenbrand, A., Marques, F. O., Catalão, J., Catita, C. M. S. & Costa, A. C. G. Large-scale active slump of the southeastern flank of Pico Island, Azores. *Geology* **40**, 939–942 (2012).
33. Hildenbrand, A. et al. Reconstructing the architectural evolution of volcanic islands from combined K/Ar, morphologic, tectonic, and magnetic data: the Faial Island example (Azores). *J. Volcanol. Geotherm. Res.* **241–242**, 39–48 (2012).
34. Hildenbrand, A., Marques, F. O. & Catalão, J. Large-scale mass wasting on small volcanic islands revealed by the study of Flores Island (Azores). *Nat. Sci. Rep.* **8**, 13898 (2018).
35. Hildenbrand, A. et al. Precise dating of large flank collapses by single-grain $^{40}Ar/^{39}Ar$ on pyroclastic deposits from the example of Flores Island (Azores). *Sci. Rep.* **14**, 11905 (2024).
36. Marques, F. O., Sibrant, A. L. R., Hildenbrand, A. & Costa, A. C. G. *Large Scale Sector Collapses in the Evolution of Santa Maria Island, Azores. Abstract V51D-2719, AGU Fall Meeting* (2013).
37. Marques, F. O., Hildenbrand, A. & Hübscher, C. Evolution of a volcanic island on the shoulder of an oceanic rift and geodynamic implications: S. Jorge Island on the Terceira Rift, Azores Triple Junction. *Tectonophysics* **738–739**, 41–50 (2018).
38. Marques, F. O., Hildenbrand, A., Costa, A. C. G. & Sibrant, A. L. .R. The evolution of Santa Maria Island in the context of the Azores Triple Junction. *Bull. Volcanol.* **82**, 39 (2020a).
39. Marques, F. O. et al. The shaping of a volcanic ridge in a tectonically active setting: the Pico-Faial Ridge in the Azores Triple Junction. *Geomorphology* **378**, 107612 (2021).
40. Costa, A. C. G., Marques, F. O., Hildenbrand, A., Sibrant, A. L. R. & Catita, C. M. S. Large-scale flank collapses in a steep volcanic ridge: Pico-Faial Ridge, Azores Triple Junction. *J. Volc. Geotherm. Res.* **272**, 111–125 (2014).
41. Costa, A. C. G., Hildenbrand, A., Marques, F. O., Sibrant, A. L. R. & de Santos, A. Catastrophic flank collapses and slumping in Pico Island during the last 130 kyr (Pico-Faial ridge, Azores Triple Junction). *J. Volc. Geotherm. Res.* **302**, 33–46 (2015).
42. Sibrant, A. L. R., Marques, F. O. & Hildenbrand, A. Construction and destruction of a volcanic island developed inside an oceanic rift: Graciosa Island, Terceira Rift, Azores. *J. Volc. Geotherm. Res.* **284**, 32–45 (2014).
43. Sibrant, A. L. R., Hildenbrand, A., Marques, F. O. & Costa, A. C. G. Volcanotectonic evolution of the Santa Maria Island (Azores): implications for palaeostress evolution at the western Eurasia-Nubia plate boundary. *J. Volc. Geotherm. Res.* **291**, 49–62 (2015).

44. Sibrant, A. L. R. et al. Morpho-structural evolution of a volcanic island developed inside an active oceanic rift: S. Miguel Island (Terceira Rift, Azores). *J. Volc. Geotherm. Res.* **301**, 90–106 (2015).
45. Sibrant, A. L. R. et al. Deformation in a hyperslow oceanic rift: insights from the tectonics of the São Miguel Island (Terceira Rift, Azores). *Tectonics* **35**, 425–446 (2016).
46. Weiß, B., Hübscher, C., Lüdmann, T. & Serra, N. Submarine sedimentation processes in the southeastern Terceira Rift / São Miguel region (Azores). *Mar. Geol.* **374**, 42–58 (2016).
47. Marques, F. O., Catalão, J. C., DeMets, C., Costa, A. C. G. & Hildenbrand, A. GPS and tectonic evidence for a diffuse plate boundary at the Azores Triple Junction. *Earth Planet. Sci. Lett.* **381**, 177–187 (2013).
48. Marques, F. O., Catalão, J. C., DeMets, C., Costa, A. C. G. & Hildenbrand, A. Corrigendum to GPS and tectonic evidence for a diffuse plate boundary at the Azores Triple Junction. *Earth Planet. Sci. Lett.* **387**, 1–3 (2014).
49. Storch, B. et al. Rifting of the oceanic Azores Plateau with episodic volcanic activity. *Nat. Sci. Rep.* **10**, 19718 (2020).
50. Ramalho, R. S. et al. Emergence and evolution of Santa Maria Island (Azores): the conundrum of uplifted islands revisited. *Geol. Soc. Am. Bull.* **129**, 372–390 (2017).
51. Miller, K. G. et al. The phanerozoic record of global sea-level change. *Science* **310**, 1293–1298 (2005).
52. Miller, K. G., Mountain, G. S., Wright, J. D. & Browning, J. V. A 180-million-year record of sea level and ice volume variations from continental margin and deep-sea isotopic records. *Oceanography* **24**, 40–53 (2011).
53. Hildenbrand, A., Gillot, P. Y., Soler, V. & Lahitte, P. Evidence for a persistent uplifting of La Palma (Canary Islands), inferred from morphological and radiometric data. *Earth Planet. Sci. Lett.* **210**, 277–289 (2003).
54. Ramalho, R. S. et al. Coastal evolution on volcanic oceanic islands: a complex interplay between volcanism, erosion, sedimentation, sea level change and biogenic production. *Earth Sci. Rev.* **127**, 140–170 (2013).
55. Marques, F. O., Hildenbrand, A., Zeyen, H., Cunha, C. & Victória, S. S. The complex vertical motion of intraplate oceanic islands assessed in Santiago Island, Cape Verde. *Geochem. Geophys. Geosyst.* 21, eGC008754 (2020).
56. Holcomb, R. T. & Searle, R. C. Large landslides from oceanic volcanoes. *Mar. Geotech.* **10**, 19–32 (1991).
57. Urgeles, R., Masson, D. G., Canals, M., Watts, A. & LeBas, T. Reccurent large-scale landsliding on the west flank of La Palma, Canary Islands. *J. Geophys. Res.* **104**, 25331–25348 (1999).
58. Deplus, C. et al. Submarine evidence for large-scale debris avalanches in the lesser antilles Arc. *Earth Planet. Sci. Lett.* **192**, 145–157 (2001).
59. Masson, D. G., Le Bas, T. P., Grevemeyer, I. & Weinrebe, W. Flank collapse and large-scale landsliding in the Cape Verde Islands, off West Africa. *Geochem. Geophys. Geosyst.* **9**, Q07015 (2008).
60. Masson, D. G. et al. Slope failures on the flanks of the western Canary Islands. *Earth Sci. Rev.* **57**, 1–35 (2002).
61. Le Friant, A., Boudon, G., Deplus, C. & Villemant, B. Large-scale flank collapse events during the activity of Montagne Pelée, Martinique, Lesser Antilles. *J. Geophys. Res.* **108**, 2055 (2003).
62. Clouard, V. & Bonneville, A. Submarine landslides in French polynesia. In *Oceanic Hotspots* (eds Hekinian, R. et al.) (Springer, 2004).
63. Hildenbrand, A., Gillot, P. Y. & Bonneville, A. Offshore evidence for a huge landslide of the northern flank of Tahiti-Nui (French Polynesia). *Geochem. Geophys. Geosyst.* **7**, Q03006 (2006).
64. Hildenbrand, A. et al. A giant volcanic island in an early Martian Ocean? *Earth Planet. Sci. Lett.* **619**, 118302 (2023).
65. *European Marine Observation Data Network (EMODnet) Bathymetry*. https://emodnet.ec.europa.eu/geoviewer/ (Accessed 09 November 2024).
66. GEBCO Compilation Group. *GEBCO 2019 Grid*. https://doi.org/10.5285/836f016a-33be-6ddc-e053-6c86abc0788e (2019).
67. Hübscher, C. & Beier, C. *Multibeam Bathymetry Processed Data (EM 120 Echosounder & Kongsberg EM 122 Dataset Compilation) of RV METEOR During Cruise M79/2, M113/1 & M128, Azores Plateau Between the Terceira Rift and the East Azores Fracture Zone*. https://doi.org/10.1594/PANGAEA.945528 (North Atlantic Ocean, PANGAEA, 2022).
68. Hübscher, C. et al.*Azores Plateau—Cruise No. M113/1—December 29, 2014—January 22, 2015—Ponta Delgada (Portugal)—Ponta Delgada (Portugal). METEOR-Berichte* 31 (DFG-Senatskommission für Ozeanographie, 2016).
69. Luis, J. F. & Miranda, J. M. Reevaluation of magnetic chrons in the North Atlantic between 35°N and 47°N: implications for the formation of the Azores Triple Junction and associated plateau. *J. Geophys. Res.* **113**, B10105 (2008).
70. Batista, L. et al. Crustal structure across the São Miguel Island (Azores, North Atlantic) and tectonic implications. *Mar. Geophys. Res.* **43**, 41 (2022).
71. Beier, C. et al. The submarine Azores Plateau: evidence for a waning mantle plume? *Mar. Geol.* **451**, 106858 (2022).
72. Kaus, B. J. P. Factors that control the angle of shear bands in geodynamic numerical models of brittle deformation. *Tectonophysics* **484**, 36–47 (2010).
73. Thielmann, M. & Kaus, B. J. P. Shear heating induced lithospheric-scale localization: does it result in subduction? *Earth Planet. Sci. Lett.* **359–360**, 1–13 (2012).
74. Olson, P., Reynolds, E., Hinnov, L. & Goswami, A. Variation of ocean sediment thickness with crustal age. *Geochem. Geophys. Geosyst.* **17**, 1349–1369 (2016).
75. del Potro, R., Hürlimann, M. & Pinkerton, H. Modelling flank instabilities on stratovolcanoes: parameter sensitivity and stability analyses of Teide, Tenerife. *J. Volc. Geotherm. Res.* **256**, 50–60 (2013).
76. Morrow, C. A., Shi, L. Q. & Byerlee, J. D. Strain hardening and strength of clay-rich fault gouges. *J. Geophys. Res.* **87**, 6771–6780 (1982).
77. Zbyszewski, G. & Ferreira, O. V. *Carta Geológica de Portugal, Ilha de Santa Maria (Açores), Scale 1:50 000* (Serviço Geológico de Portugal, 1960).
78. Watt, S. F. The evolution of volcanic systems following sector collapse. *J. Volc. Geotherm. Res.* **384**, 280–303 (2019).
79. Walter, T. R. et al. Rift zone reorganization through flank instability in ocean island volcanoes: an example from Tenerife, Canary Islands. *Bull. Volcanol.* **67**, 281–291 (2005).
80. Weiß, B., Hübscher, C. & Lüdmann, T. The tectonic evolution of the south-eastern Terceira rift / São Miguel Region (Azores). *Tectonophysics* **654**, 75–95 (2015).
81. Weiß, B., Hübscher, C., Wolf, D. & Lüdmann, T. Submarine explosive volcanism in the southeastern Terceira Rift/São Miguel Region (Azores). *J. Volc. Geotherm. Res.* **303**, 79–91 (2015).
82. Beier, C. et al. Extreme intensity of fluid-rock interaction during extensive intraplate volcanism. *Geochim. Cosmochim. Acta* **257**, 26–48 (2019).
83. Chang, Y. C. et al. Asymmetric abundances of submarine sediment waves around the Azores volcanic islands. *Mar. Geol.* **449**, 106837 (2022).
84. Huppert, K. L., Royden, L. H. & Perron, J. T. Dominant influence of volcanic loading on vertical motions of the Hawaiian Islands. *Earth Planet. Sci. Lett.* **418**, 149–171 (2015).
85. Turcotte, D. L. & Schubert, G. *Geodynamics* (Cambridge University Press, 2002).
86. Spieker, K., Rondenay, S., Ramalho, R., Thomas, C. & Helffrich, G. Constraints on the structure of the crust and lithosphere beneath the Azores Islands from teleseismic receiver functions. *Geophys. J. Int.* **213**, 824–835 (2018).
87. Romer, R. H. W., Beier, C., Haase, K. M., Eberts, A. & Hübscher, C. The evolution of central volcanoes in ultraslow rift systems: Constraints from D. João de Castro seamount, Azores. *Tectonics* **40**, e2020TC006663 (2021).
88. Marques, F. O., Hildenbrand, A., Victória, S. S., Cunha, C. & Dias, P. Caldera or flank collapse in the Fogo volcano? What age? Consequences for risk assessment in volcanic islands. *J. Volc. Geotherm. Res.* **388**, 106686 (2019).

89. Robinson, J. E. & Eakins, B. W. Calculated volumes of individual shield volcanoes at the young end of the Hawaiian Ridge. *J. Volc. Geotherm. Res.* **151**, 309–317 (2006).
90. Le Friant, A. et al. Submarine landslides around volcanic islands. In *Submarine Landslides* (eds Ogata, K. et al.) (2019).
91. Merle, O. & Borgia, A. Scaled experiments of volcanic spreading. *J. Geophys. Res.* **101**, 13805–13817 (1996).
92. van Wyk, B. et al. The role of basement in volcano deformation. In: McGuire, W.J. Eds., Volcano instability on the earth and other planets. *Geol. Soc. Lond. Spec. Publ.* **110**, 95–110 (1996).
93. van Wyk, B. & Matela, R. J. Styles of volcano-induced deformation: Numerical models of substratum flexure, spreading and extrusion. *J. Volc. Geotherm. Res.* **81**, 1–18 (1998).
94. Owen, S. et al. Rapid deformation of Kilauea volcano: global positioning system measurements between 1990 and 1996. *J. Geophys. Res.* **105**, 18983–18998 (2000).
95. Smith, J. R., Malahoff, A. & Shor, A. N. Submarine geology of the Hilina slump and morpho-structural evolution of Kilauea volcano, Hawaii. *J. Volc. Geotherm. Res.* **94**, 59–88 (1999).
96. Hübscher, C. *Marine Multichannel Seismic Data Collected During RV METEOR Expedition M113*. https://doi.org/10.5281/zenodo.11394390 (University of Hamburg, 2024).

Acknowledgements

A.C.G. Costa benefited in 2014-2016 from a Humboldt Post-Doc Research Fellowship (Alexander von Humboldt Foundation, Germany). We thank Miguel Souto for the expert help in the production of the bathymetric and backscatter images. The final version of the manuscript benefitted from the insightful and constructive reviews of Luca Cocchi and Darin Schwartz, and the professional handling of the manuscript by Masaki Yoshida.

Author contributions

FOM designed and was the PI of the project, collected the new field data, analysed field and geophysical data, and wrote and revised the manuscript; LPR processed the bathymetry, analysed data, wrote her part of the manuscript, and revised the text; CH took care of the seismic data, analysed data, wrote his part of the manuscript, and revised the text; ACGC took care of the numerical modelling, analysed data, wrote her part of the manuscript, and revised the text; AH collected field data, carried out the geochronology, analysed all data, and revised the text.

Declarations

Competing interests

The authors declare no competing interests.

Additional information

Supplementary Information The online version contains supplementary material available at https://doi.org/10.1038/s41598-025-87191-5.

Correspondence and requests for materials should be addressed to F.O.M.

Reprints and permissions information is available at www.nature.com/reprints.

Publisher's note Springer Nature remains neutral with regard to jurisdictional claims in published maps and institutional affiliations.